Journal Pre-proof

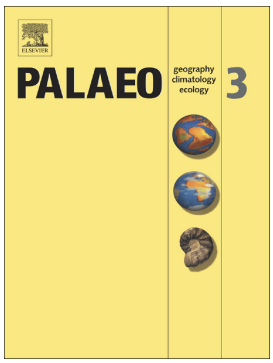

Response of the Akrotiri Marsh, island of Cyprus, to Bronze Age climate change

Calian J. Hazell, Matthew J. Pound, Emma P. Hocking

PII: S0031-0182(21)00573-3

DOI: https://doi.org/10.1016/j.palaeo.2021.110788

Reference: PALAEO 110788

To appear in: *Palaeogeography, Palaeoclimatology, Palaeoecology*

Received date: 17 August 2021

Revised date: 4 December 2021

Accepted date: 4 December 2021

Please cite this article as: C.J. Hazell, M.J. Pound and E.P. Hocking, Response of the Akrotiri Marsh, island of Cyprus, to Bronze Age climate change, *Palaeogeography, Palaeoclimatology, Palaeoecology* (2021), https://doi.org/10.1016/j.palaeo.2021.110788

Response of the Akrotiri Marsh, island of Cyprus, to Bronze Age climate change

Calian J Hazell*, Matthew J Pound and Emma P Hocking

Department of Geography & Environmental Sciences, Northumbria University, Newcastle upon Tyne, NE1 8ST, UK

*Corresponding author contact information: email- calian.j.hazell@northumbria.ac.uk; address- Department of Geography & Environmental Sciences, Ellison Building, Northumbria University, Newcastle upon Tyne, NE1 8ST, United Kingdom

Abstract

Here we present two multiproxy records covering the last 5000 years from the Akrotiri Marsh in southern Cyprus. Pollen and diatom analysis of radiocarbon dated marsh sediments with an average chronological resolution of one date every thousand years, reveal expansion and contraction of the marsh in response to mid-late Holocene climate events, with peak aridity reconstructed in the early Bronze Age, inferred between 4.3 and 4.1 cal ka BP, and repeated dry intervals in the Late Bronze Age, inferred between 3.4 and 3.1 cal ka BP. The record provides important contextual climate data to the debate surrounding reported Early and Late Bronze Age societal collapse events present in numerous archaeological archives throughout the Mediterranean and Near Eastern region. This is the first multiproxy record from the island of Cyprus potentially displaying the 4.2 ka BP event. The characteristics of the inferred 3.2 ka BP event are very similar to the manifestation of the event in the east of Cyprus and on the southern Levantine mainland. These results contribute to the regional understanding of Bronze Age climates on Cyprus, give insight into the expression of global climate forcing mechanisms such as the North Atlantic Oscillation and the Siberian High, and provide potential evidence for reduced anthropogenic land-use during the 4.2 ka BP and 3.2 ka BP Events supporting what is documented in archaeological archives.

Keywords: Pollen, diatoms, 4.2 ka BP Event, 3.2 ka BP Event, palaeoenvironmental change.

1. Introduction

Climate change has been proposed as a major driver of societal collapse during the Bronze Age of the eastern Mediterranean, with two key periods of decline and collapse having been identified in the archaeological record - the Early Bronze Age collapse (Weiss and Courty, 1993; Weiss et al., 1993; Cooper, 1997; Nigro, 2000; Kennedy, 2016; Weiss, 2017) at ca. 4.45 to 3.95 cal ka BP (Kennedy, 2016), and Late Bronze Age collapse (Weiss, 1982; Bryce, 2005; Cohen and Singer, 2006; Knapp, 2011; Kaniewski et al., 2013; Cline, 2014; Langgut et al., 2014; Knapp and Manning, 2016) at ca. 3.20 to 3.05 cal ka BP (Cline, 2014; Knapp et al., 2016; Weiss, 1982). Palaeoenvironmental research has linked each of these intervals of politico-economic decline and settlement abandonment with specific climatic events (Carpenter, 1966; Neumann and Parpola, 1987; Weiss et al., 1993; Weiss, 1997; Tarasov et al., 1998; Cullen and DeMenocal, 2000; Kaniewski et al., 2008, 2010, 2013, 2015; Roberts et al., 2011; Drake, 2012; Langgut et al., 2013, 2015; Kennedy, 2016). The climatic event often associated with the Early Bronze Age collapse is termed the 4.2 ka BP event, whereby the statistical analysis of nearly 50 proxy records suggests a Mediterranean-wide period of centennial scale climate change from 4.50 – 4.20 cal ka BP (Finné et al., 2019), and extending up to 3.80 cal ka BP in some records (Bini et al., 2019). The 4.2 ka BP event in the archaeological records is associated with the collapse and settlement disruption events that began on the plains of Jezireh at ca. 4.20 cal ka BP and became region-wide by ca. 4.00 cal ka BP (Kennedy, 2016). The end of Early Bronze Age urban culture in the southern Levant might have begun earlier at ca. 4.50 cal ka BP (Höflmayer, 2017). The climatic event often associated with the Late Bronze Age collapse is termed the 3.2 ka BP event. This event occurred in two distinct parts, the first comprising a cold and arid interval from 3.50 – 3.30 cal ka BP (Kaniewski et al., 2008, 2010; Finné et al., 2019) and a second cold interval that typically featured a three-pulse ("W-shaped") arid-wet-arid event between 3.35 – 2.80 cal ka BP (Drake, 2012; Kaniewski et al., 2013, 2019). Despite widespread palaeoenvironmental evidence for climate change during both of these events, it is not the only proposed cause of these societal collapse events. Individual site destruction or region-wide disruption has been attributed to tsunamis and earthquakes, destabilisation of centralised economies, collapse of international trade and foreign invasion (Cline, 2014; Kennedy, 2016; Knapp and Manning, 2016). It should also be considered that all of these causes of collapse can both be influenced by climatic change and influence a societal response to changing climates.

Three main external climate-forcing mechanisms are often cited as controlling the distribution of Mediterranean climates throughout the different seasons, the Intertropical Convergence Zone/African-Arabian/Asian monsoon 2.3-2.5 kyr summertime cycle (Russell et al., 2003; Alpert et al., 2006), the continental 2.3 kyr Siberian High winter/spring cycle (Rohling et al., 2002; Roberts et al., 2012), and the maritime 1.5 kyr North Atlantic Oscillation wintertime cycle (Bond, 1997; Bond et al., 2001; Rohling et al., 2002; Davis and Brewer, 2009). It has been documented that throughout the Holocene, a positive NAO accompanies a relatively cold and dry winter climate across the northern Mediterranean borderlands (López-Moreno et al., 2011; Di Rita et al., 2018), northern Italy and the Balkans between 43° and 45°N (Di Rita and Magri, 2019; Isola et al., 2019), and the Aegean (Katrantsiotis et al., 2019). Typically in the Levantine region, more emphasis is given to the effects of the continental Siberian High cycle (Lingis and Michaelides, 2009; Geraga et al., 2010), the African-Arabian monsoon cycles (Baioumy et al., 2010; Triantaphyllou et al., 2014), or a combination of both regimes (Jalut et al., 2009; Desprat et al., 2013).

Cyprus, as a semi-arid island, has been identified as an area where biodiversity and agriculture are facing a triple threat from future climate change (Vogiatzakis et al., 2016). A combination of increasing temperatures and decreasing precipitation threatens the lowland vegetation and agriculture through water scarcity and shifting human activity, whilst the mountain ecosystems of the Troodos are subject to altitudinal pressures from warming (Vogiatzakis et al., 2016). This vulnerability to temperature and precipitation variability likely existed throughout the Holocene and may be a contributing factor to societal collapse on Cyprus in the late Bronze Age (Kaniewski et al., 2013). The early Bronze Age collapse, 4.2 ka BP event (4.50 – 4.20 cal ka BP), would fall within the Philia Phase on Cyprus (Kearns and Manning, 2019; Supplementary Table S1). When compared to the preceding Chalcolithic, this is a time interval of a myriad of cultural, material and social innovations that marks a distinct change in the island's archaeological record (Knapp, 2008). The degree of archaeological change has led to inferences of ethnic migration to the island, which Catling, (1975) attributed to Early Bronze Age refugees from Anatolia (Knapp, 2008). Palaeoenvironmental records on Cyprus come primarily from sedimentological, shallow marine faunas and pollen analysis (e.g. Morhange et al., 2000; Kaniewski et al., 2013; Ghilardi et al., 2015). On Cyprus, palynological research was initially conducted as a minor supplement to books documenting archaeological surveys on the island for landscape reconstruction (e.g. Bottema, 1966, 1976; Renault-Miskovsky, 1985; Renault-Myskovsky, 1989). More recently, palynological research has been conducted to investigate climatic and environmental change, at the Akrotiri (Limassol) Salt Lake (Allen et al., 2009), the Larnaca Salt Lake/Hala Sultan Tekke (Kaniewski et al., 2013; 2020), and a terrestrial shaft at the nearby

coastal site of Pyla *Kokkinokremnos* (Kaniewski et al., 2019). Pollen records from near Larnaca have shown both the 4.2 ka BP and 3.2 ka BP events (Kaniewski et al., 2020). The Larnaca Salt Lake record shows a temperature anomaly of ~ -2.5°C at 4.2 cal ka BP and 3.15 cal ka BP (Kaniewski et al., 2020). This record and the nearby Pyla *Kokkinokremno* site show a three-pulse ("W-shaped" – original author term) arid-wet-arid event, with increased aridity at ca. 3.15 cal ka BP and ca. 2.90/2.85 cal ka BP framing a wetter period from ca. 3.00 – 2.95 cal ka BP (Kaniewski et al., 2019; 2020). This corresponds to widespread abandonment of sites and the destruction of monumental structures at the end of the Second Late Cypriot Period (Knapp, 2013; Knapp and Manning, 2016). By contrast, a pollen record from the Akrotiri Peninsula does not display any climatic event during the Bronze Age due to inadequate dating resolution (Allen et al., 2009). Presently, there are no Holocene diatom studies known from Cyprus that might also contribute to our understanding of hydrology during these Bronze Age climate events. The 4.2 ka BP and 3.2 ka BP events are present in records from around Larnaca on Cyprus and that there was also an island-wide societal shift at the end of the Late Bronze Age. However palaeoenvironmental research is lacking for the rest of the island meaning any potential relationships between archaeological events and environmental change is reliant on extrapolation from the Larnaca coastal region. We therefore need more detailed and geographically-widespread climate reconstructions from Cyprus that allow improved understanding of both Bronze Age, and wider Holocene, palaeoenvironments that can provide context to archaeological records.

This paper seeks to provide the first multiproxy Bronze Age record on Cyprus, from a previously unstudied environmental archive in southern Cyprus, in order to provide the opportunity to identify and better understand the 4.2 ka BP and 3.2 ka BP climatic events on the island. The aim is to provide a climatological context to the Cypriot Bronze Age, allowing for future comparison to local archaeological records, and therefore improving our understanding of potential climate-societal relationships in the Mediterranean Bronze Age.

2. Study area

The island of Cyprus has a Mediterranean climate of hot, dry summers and relatively mild, moist winters (Delipetrou et al., 2008; Fall, 2012). The distribution of modern vegetation and climate patterns are primarily controlled by topographical variation across the island (Pantelas, 1996; Delipetrou et al., 2008; Fall, 2012); two mountain ranges, the Troodos (1950 m peak) and the Kyrenia Range (1000 m peak), create high elevation moist environments by drawing up and condensing moist air off the Mediterranean Sea. Pollen taxa on the island demonstrate clear

relationships with climatic variables allowing for a strong basis for interpreting palaeoenvironmental records from the island (Pantelas, 1996; Fall, 2012). The Akrotiri Peninsula is the southernmost point of the island of Cyprus, most of the peninsula lies within the British Overseas Territory of the Sovereign Base Areas of Akrotiri and Dhekelia (Fig. 1). The peninsula is dominated by the Limassol Salt Lake with two smaller freshwater marshes, Phassouri/Fassouri (here termed Akrotiri) and Zakaki to the northwest and northeast (Birol et al., 2011), which collectively form the Akrotiri wetlands Special Protection Area (Kassinis and Charalambidou, 2021). The hydrology of the Akrotiri Marsh is controlled by precipitation and by groundwater coming from the Akrotiri Aquifer, which is part of the Kouris River basin (Birol et al., 2011). The strong precipitation control, both directly and indirectly from groundwater, means this study site is particularly sensitive to periods of drought and aridity (Birol et al., 2011).

[Insert Figure 1]

3. Materials and methods

Six cores were retrieved from the Akrotiri Marsh (34°37'54.3"N, 32°55'59.5"E; 34.631740"N, 32.933184"E) with a Russian peat corer in March 2018, and two were selected for microfossil proxy analysis. Sediments were analysed for pollen and diatoms (92 samples each) and dated using AMS radiocarbon dating. Core AM18-1 was sampled at 4 cm resolution, increasing to 0.5 cm resolution through the Bronze Age section of the core, specifically the Protohistoric Bronze Age II and Protohistoric Bronze Age III of Knapp (2008) (Supplementary Table S1). Core AM18-5 was sampled at 1-4 cm resolution through the Late Chalcolithic to Byzantine Age peat unit (unit 6 of Fig. 2). Materials that were appropriate for radiocarbon dating (above ground plant fragments, wood) were selected for radiocarbon dating and analysed at the Gliwice Absolute Dating Methods (GADAM) Centre in the Silesian University of Technology, Poland. Raw radiocarbon results (uncalibrated ^{14}C years) were calibrated using the IntCal13 calibration curve in the R software computing environment ("R Core Team T," 2017) using the Bacon package (Blaauw and Christen, 2019) and reported to 95.4% confidence intervals. Age-depth models were also produced by the Bacon package using a Bayesian statistical modelling method by estimating an implicit variable accumulation rate assuming a gamma distribution pattern. By dividing the core into varying numbers of vertical sections (a variable manually programmed by the user allowing for the visual

inspection of numerous outputs) Bacon processes millions of Markov Chain Monte Carlo (MCMC) iterations in order to estimate the accumulation rate (in years/cm) for each of these sections (Blaauw and Christen, 2019). The calculated variable accumulation rate is then compared to the calibrated radiocarbon date points for accuracy, allowing for re-calculation using different accumulation rate internal variables - “accumulation shape” and “accumulation mean” (Blaauw and Christen, 2019). For core AM18-1, forty-one 5 cm sections were analysed, with an optimal accumulation shape value of 1.5, and an optimal accumulation mean value of 20. For core AM18-5, eighteen 10 cm sections were analysed, with an optimal accumulation shape value of 1.5, and an optimal accumulation mean value of 50. For both cores, the optimal “memory strength” value was 4, and the optimal “memory mean” value was 0.7.

Samples for pollen analysis were spiked with *Lycopodium clavatum* tablets to enable pollen concentration calculation and 10% hydrochloric acid (HCl) was used to dissolve each tablet and remove carbonates. Samples were then treated with 10 ml of 10% Potassium hydroxide (KOH digestion) in a 80°C water bath for 4 minutes to disperse the material, and sieved at 125 µm. Following this, silicates were removed using 10 ml of 48% hydrofluoric acid and flushed with HCl. Acetolysis was conducted, in order to dissolve any remaining unwanted organic content in the samples, by washing with 10 ml Glacial Acetic Acid (GAA), heating for 3 minutes in a 9:1 ratio of Acetic Anhydride to Sulphuric acid, followed by a second GAA rinse. Samples were then sieved at 10 µm to remove residual clay material, rinsed with Isopropyl Alcohol, and mounted onto a glass microscope slides in silicone oil. Pollen taxonomic identification was achieved using a variety of sources (Bouchal et al., 2016, 2017; Chester and Raine, 2001; Cugny et al., 2010; Demiskova et al., 2013; *“PalDat – a palynological database,”* 2000; El-Amier, 2015; Gelorini et al., 2011; Martin and Harvey, 2017; Poliakova and Behling, 2016; Praglowski, 1962; Shubharani et al., 2013; Stebler, 2015; Van Geel, 1972; Van Wichelen et al., 1999; Willard et al., 2004; Yildiz, 2006; Yildiz et al., 2009).

Samples for diatom analysis were initially sieved at 10 µm to remove clay and then processed in 20 ml of 30% hydrogen peroxide solution at 80°C until all non-silicate material is dissolved (Battarbee, 1986; Battarbee et al., 2001). Residues were then mounted onto glass slides using the affixant Naphrax. Pollen and diatoms were analysed under a Leica DM2500 LED light microscope, with a target minimum of 300 pollen grains and 300 diatom valves counted per sample. Following the generation of a modern day Cypriot diatom taxonomy list (Kelly et al., 2012; Álvarez-Blanco and Blanco, 2014; Cantonati et al., 2016, 2018; Stocchetti et al., 2016), fossil diatom identification was achieved using a variety of photographic sources (Álvarez-Blanco and Blanco, 2014; Bahls et al., 2018; Blanco, 2016; *"iNaturalist Diaton Database"*, 2013; *Ministère de*

la Transition écologique et Solidaire, 2019; *Office International de l'Eau*, 2017; *"Diatoms of North America"*, 2017; Delgado et al., 2013; Guiry and Guiry, 2020; Jüttner et al., 2017; Krammer and Lange-Bertalot, 1986, 1991; Lange-Bertalot, 2001; Lange-Bertalot and Metzeltin, 1996; Mora et al., 2017; Morales et al., 2009; Ohtsuka et al., 2009; Otsuka, 2018; Potapova et al., 2016; Pullan, 2003; Reichardt, 2011; Solak et al., 2016; Swedish Meterological and Hydrological Institute, 2018).

Pollen counts were transformed into relative percentages for each sample depth in order to compare abundance fluctuations through time, and pollen concentrations were calculated for each sample by counting *Lycopodium* grains alongside pollen quantities, enabling confirmation that percentage fluctuations are genuine representations of pollen assemblage turnover and not statistical artefacts. This data was tabulated and visualised in TILIA software version 2.0.41 (Grimm, 2011). Stratigraphically constrained cluster analysis using the incremental sum of squares method provided by the CONISS program was used to identify statistically significant assemblage changes and determine proxy zones (Grimm, 1987), with no zones being identified below a sum of squares value of 7. Pollen vegetation taxa ecological inferences follow Kaniewski et al., (2013), with further ecological inferences, such as water availability, made using Brullo et al., (2005), Fall, (2012), Gucel et al., (2012, 2013), and Hadjichambis et al., (2004). As a result of the lack of Holocene diatom research on Cyprus there is no tailored diatom training set for allowing palaeoenvironmental inferences from analogous modern day settings, an issue that extends to the rest of the eastern Mediterranean (Woodbridge and Roberts, 2011). In order to draw meaningful environmental interpretation from fossil assemblages, fossil diatom taxa are identified, quantified, and related to the modern day ecologies of those species present (Battarbee et al., 1998; Juggins, 2001; Reed et al., 2001).

4. Results

4.1. Radiocarbon results

The chronology comes from six radiocarbon dates, three from each core AM18-1 and AM18-5 (Table 1; Fig. 2). Five additional dates were discounted from age modelling, specifically four from AM18-1 and one from AM18-5 (Table 1). Two of these were discounted (GdA-6013, 5664) as modern day ages were reported, which cannot be possible due to the sample depths. It is likely these samples were contaminated by

modern plant root material. Two bulk sediment ages from the peat unit (GdA-5871, 6010) appear to have been contaminated by 'old' carbon, which is a known issue in dating bulk peat material (Shore et al., 1995; Fahmi et al., 2021), and a bulk sediment age from the organic clay unit underlying the peat returned an anomalously young age, assumed to be due to percolation of humic acid. Supplementary Table S2 provides the complete Bacon age-depth modelling output data for both cores, including the full range of potential dates, however unlikely, at each centimetre depth interval.

[Insert Table 1, and Figure 2]

Core AM18-1 features an average chronology resolution of one sample every 33 cm, or 1043 years, through the dated length, while core AM18-5 features an average chronological resolution of one sample every 18 cm, or 1083 years, through the dated length. This is not a high-resolution chronological dataset, and the study would have benefit from the greater occurrence of datable radiocarbon material. Furthermore, as with any radiocarbon analyses, the 95.4% ranges used in calibration and the final statistically generated age-model each feature inherent uncertainties and limitations (e.g. Table 1 "Calibrated age range" column, Supplementary Table S2 "Minimum" and "Maximum" cal yrs BP ranges). Despite this, the confidence in these age-depth models is relatively high. This is because only the most reliable material was selected for production of the age model diagrams, and as such it is the opinion of the authors that any future addition of more radiocarbon dates would be unlikely to cause a dramatic shift in the age model, but instead provide a finer resolution chronology and a more robust age model.

This study and its results may therefore be considered an initial study at this site, in the interest of gathering contextual data that can be compared and correlated with past and future climatic and archaeological Cypriot research. While the positive correlation between our age-depth model derived mean dates and the dating of identical inferred climatic events on southern and eastern Cyprus adds support to the chronological accuracy, all dates are based on this current age-model, and therefore must be viewed with the associated uncertainty and date ranges identified in Table 1 and Supplementary Table S2 in mind. For added clarity, the precise radiocarbon data points and their ranges are added to the lithology axis of each Figs. 3, 4, 5 and 6.

4.2. Pollen analysis

Environmental summary diagrams for pollen analysis are presented for cores AM18-1 (Fig. 3) and AM18-5 (Fig. 4). The corresponding full taxonomic pollen diagrams are available online in supplementary figures S1, S2 and S3. Results are described by Pollen Assemblage Zone (*PAZ*).

[Insert Figures 3 and 4]

4.2.2. Core AM18-1

PAZ-1: 4.85 to 3.38 cal ka BP (150-95 cm)

Wetland marsh and bog taxa (63.3 – 16.8%), Mediterranean woodland (24.7 – 8.9%) and dry steppe taxa (42.6 – 0%) dominate PAZ-1 (Fig. 3). The relative abundance of wetland taxa decrease from 50 to 17% between 4.50 and 4.30 cal ka BP, before increasing through to the top of the zone (Fig. 3). Conversely, Mediterranean woodland taxa, largely driven by Cupressaceae, increase up to ca. 4.10 cal ka BP (15 - 24.5%) and decrease towards the top of the zone (4%) (Fig. 3). After recording initial low relative abundances up to ca. 4.50 cal ka BP, dry steppe taxa begin to increase in relative abundance largely driven by pollen of the Cichorieae, which peak in abundance between ca. 4.33 – 4.10 cal ka BP (20-41%) and at ca. 3.40 cal ka BP (37%). During the initial interval of low dry steppe between ca. 4.85 – 4.50 cal ka BP, the cultivated species and weeds group forms 5 – 11% of the assemblage, before a decrease to 2% between ca. 4.50 – 4.00 cal ka BP as dry steppe expands (Fig. 3). At the start of this zone the fen trees and riverine forest taxa group form 10% of the pollen and spore assemblage (Fig. 3). The presence of pollen assigned to this group then decreases in the record until it is absent between 4.40 – 4.20 cal ka BP, coincident with the peak in dry

steppe taxa (Fig. 3). As the wetland marsh and bog group increases in relative abundance, following this peak in dry steppe taxa, first the deciduous oak grove group returns to the record and then the fen trees and riverine forest groups return (Fig. 3).

PAZ-2: 3.38 to 3.15 cal ka BP (95-86 cm)

PAZ-2 is dominated by the pollen and spores of taxa characteristics of wetland marsh and bog (Fig. 3). These pollen and spores form >40% of the assemblage with the exception of two short intervals at 3.33 cal ka BP and 3.20 – 3.15 cal ka BP (Fig. 3). The first of these intervals shows an increase in dry steppe taxa (20.5-39%) and cultivated species and weeds (4%) (Fig. 3). Whilst the second, and longer interval, of decreased wetland marsh and bog taxa is marked by the dominance of Mediterranean woodland taxa (55-74%) and low relative abundances (0.5%) to complete absence of cultivated species and weeds (Fig. 3). Between these two minima in wetland marsh and bog taxa are sporadic occurrences of fen trees and riverine forest taxa and deciduous oak grove taxa (1-2% and 0.7% respectively).

PAZ-3: 3.15 to 2.40 cal ka BP (86-65 cm)

The first few centimetres of PAZ-3 show an increase in wetland marsh and bog taxa following the peak of the Mediterranean woodland group at the end of PAZ-2 (Fig. 3). This culminates at 2.97 cal ka BP with wetland marsh and bog taxa forming 61% of the total assemblage, Mediterranean woodland a further 21% and deciduous oak groves and fen trees and riverine forests groups 7% (Fig. 3). This is followed by a decrease in wetland marsh and bog to 28.5% of the assemblage, deciduous oak groves (0.8%) and fen trees and riverine forests absent at 2.70 cal ka BP (Fig. 3). Initially, this decrease also includes Mediterranean woodland taxa which decrease from 21% of the assemblage at 3.00 cal ka BP to 9% at 2.80 cal ka BP and an increase in dry steppe taxa to 23% (Fig. 3). However, by 2.70 cal ka BP Mediterranean woodland taxa (28%) are more abundant than the dry steppe group (16%) (Fig. 3). There then follows an increase in wetland marsh and bog, deciduous oak groves, fen trees and riverine forests, moist forbe-grass and meadow steppe and cultivated species and weeds environmental groups towards the top of PAZ-3 at the expense of the dry steppe group (Fig. 3).

PAZ-4: 2.40 cal ka BP to present (65 cm-top)

The final zone of core AM18-1 is interrupted by core loss between 60 and 50 cm, an interval barren of palynomorphs from at least 24 to 20 cm and potentially as large as 27 to 17 cm, and two samples with poor pollen preservation at 36 and 16 cm (Fig. 3). Despite this disjointed nature, PAZ-4 begins with a continuation of the increase in wetland marsh and bog, deciduous oak groves and fen trees and riverine forests that characterised the top of PAZ-3 (Fig. 3). With deciduous oak groves reaching 17% at 2.25 cal ka BP, whilst cultivated species and weeds become absent (Fig. 3). Following a 10 cm section of core loss, a period of decreasing abundance of wetland marsh and bog, deciduous oak groves and fen trees and riverine forests pollen and spore taxa culminates at 1.70 cal ka BP with a peak in abundance of the dry steppe group of 19% (Fig. 3). After 1.50 cal ka BP, the sedimentology of core AM18-1 changes and the pollen and spore record becomes less continuous with interruptions caused by poor preservation and absence (Fig. 3). A shift in abundance from Mediterranean woodland to wetland marsh and bog and a decrease in dry steppe and cultivated species and weeds groups can be seen from 1.34 to 1.25 cal ka BP (Fig. 3). A final peak of wetland marsh and bog taxa is also seen at 0.85 cal ka BP, before an increase in Mediterranean woodland and taxa with wide environmental tolerances towards the top of the core (Fig. 3).

4.2.3. AM18-5

PAZ-1: 4.90 to 3.99 cal ka BP (84-64 cm)

Unlike AM18-1, PAZ-1 in AM18-5 is less dominated by the wetland marsh and bog group (Fig. 4). Whilst the oldest sample at 4.90 cal ka BP comprises 67% of pollen and spore taxa attributed to the wetland marsh and bog group, this decreases to 13.5% by 4.77 cal ka BP, with increases in Mediterranean woodland, dry steppe and cultivated species and weeds groups (Fig. 4). wetland marsh and bog taxa recover to 28% at 4.65 cal ka BP, at the expense of dry steppe taxa (Fig. 4). This peak leads into an interval from 4.58 to 4.20 cal ka BP when the wetland marsh and bog group accounts for ≤10% of the assemblage and there are high relative abundances of Mediterranean woodland and dry steppe

groups. MarshFrom 4.20 cal ka BP to the top of the zone, wetland marsh and bog group taxa increase in abundance, initially at the expense of dry steppe taxa and alongside an increase in the Mediterranean woodland group up to ca. 4.10 cal ka (Fig. 4). Pollen and spores assigned to the deciduous oak groves and fen trees and riverine forests groups have a sporadic occurrence throughout most of PAZ-1 until 4.00 cal ka BP (Fig. 4). The top of PAZ-1 is constrained by an interval of core loss from ca. 4.00 – 3.00 cal ka BP (Fig. 4).

PAZ-2: 3.01 to 2.00 cal ka BP (49-32 cm)

PAZ-2 begins with increasing amounts of pollen and spores attributed to the wetland marsh and bog group from 31% at 3.01 cal ka BP to 63.5% at 2.83 cal ka BP (Fig. 4), and notable presence of taxa attributed to the moist forbe-grass and meadow steppe group (Fig. 4). It is then followed by a brief reappearance of cultivated species and weeds taxa, including the only Late Bronze Age occurrence of *Cerealia* in core AM18-5 (18%) at 2.78 cal ka BP (Fig. 4, Figure S3). deciduous oak groves taxa decrease in absence during the interval of increasing wetland marsh and bog group, but reappears at 2.78 cal ka BP (Fig. 4). The fen trees and riverine forests group increases in abundance from 2.78 to 2.56 cal ka BP, and then decreases, along with the wetland marsh and bog group to a minimum at 2.33 cal ka BP (Fig. 4). There is a 10% increase in dry steppe taxa at 2.33 cal ka BP, and also a 10% increase in taxa with wide environmental tolerances (Fig. 4). From 2.33 cal ka BP to the top of PAZ-2 there are increases in the wetland marsh and bog group, the fen trees and riverine forests group and the moist forbe-grass and meadow steppe group (Fig. 4).

PAZ-3: 2.00 to 1.38 cal ka BP (32-18 cm)

The final zone of core AM18-5 is dominated by the Mediterranean woodland group, which accounts for 62% of the assemblage at 1.90 cal ka BP (Fig. 4), and relatively high amounts of the deciduous oak groves, which reaches 13-15.5% at 1.90-1.78 cal ka BP, and fen trees and riverine forests groups (Fig. 4). These increased abundances occur at the expense of the formerly high amounts of pollen in the wetland marsh and bog group present at the end of PAZ-2, which now decrease to a minimum of 9% at 1.90 cal ka BP, while the moist forbe-grass and

meadow steppe group is also briefly absent from the record (Fig. 4). Following this the wetland marsh and bog group increases to 21% by 1.55 cal ka BP that is coincident with a final peak in the fen trees and riverine forests group (Fig. 4). By 1.49 cal ka BP, the pollen assemblage is dominated by Mediterranean woodland taxa and whilst the wetland marsh and bog group increases towards the top of the core, the dry steppe group remains a minor component of the assemblage (Fig. 4).

4.3. Diatom analysis

Ecological summary diagrams for diatom analysis are presented for cores AM18-1 (Fig. 5) and AM18-5 (Fig. 6). The corresponding full taxonomic diatom diagrams are available online in supplementary files Fig. S4 and S5. Results are described by Diatom Assemblage Zone (*DAZ*). Diatom ecology inferences for taxa with >5% abundance in at least one sample are summarised in Supplementary Table S3. Any further supporting literature for diatom ecology inferences are cited in the text of the discussion.

[Insert Figures 5 and 6]

4.3.2. Core AM18-1

Barren: 4.85 to 3.73 cal ka BP (148-108 cm)

DAZ-1: 3.73 to 3.21 cal ka BP (108-88 cm)

Fresh-brackish taxa and oligosaprobus (high water quality) taxa, in particular *Epithemia argus*, generally make up the majority of the diatom assemblage throughout the core. In DAZ-1, after an initial decline in percentage abundance from ca. 3.70 cal ka BP there is an expansion in these groups at ca. 3.35 cal ka BP, followed by a second decreasing phase to the top of the zone at ca. 3.22 cal ka BP (Fig. 5). Marine and brackish-marine taxa record an inverse signal, increasing through to 3.40 cal ka BP, decreasing at ca. 3.35 cal ka BP, and increasing again to

the top of DAZ-1 (Fig. 5). The temporary inversion in trends at ca. 3.35 cal ka BP is approximately coincident with the boundary between the traditional archaeological intervals Late Cypriot IIA and IIB (Supplementary Table S1). Following this boundary freshwater taxa also increase in representation, indicating a highly sensitive environment. Taxa suggestive of a more trophic environment initially mirror the trend in taxa preferring higher salinities, increasing up to 3.40 cal ka BP, decreasing at ca. 3.35 cal ka BP, and increasing again up to ca. 3.30 cal ka BP (Fig. 5). After this point however, relative abundances of oligosaprobic taxa increase through to the top of the zone (Fig. 5). Other ecological trends following ca. 3.35 cal ka BP suggest a more nitrogen rich, alkaline, and oxygen depleted environment (Fig. 5).

DAZ-2: 3.21 to 3.10 cal ka BP (88-84 cm)

The continued expansion of higher salinity environments are observed in DAZ-2, with relatively low abundances of *Epithemia argus* and *Ulnaria vitrea*, while *Paralia sulcata* and *Diploneis bombus* abundances remain elevated (Fig. 5). The further reduction of oxygen saturation and the continuation of eutrophic and elevated nitrogen conditions are also suggested by diatom assemblages (Fig. 5). *Navicula oblonga* is a species sensitive to human impacts (Biological Condition Gradient [BCG] category 3) (Davies and Jackson, 2006; Sutula et al., 2016) and remains elevated in DAZ-2, while taxa tolerant of human disturbance (the BCG category 5) record decreased percentage relative abundances (Fig. 5). This may indicate reduced human impact on the landscape.

DAZ-3: 3.10 cal ka BP to present (84-0 cm)

At the onset of DAZ-3, salinity is inferred to decrease, which continues throughout the remainder of the Bronze Age (Fig. 5). Taxa tolerant of human disturbance (BCG category 5) also recover at the base of this zone at ca. 3.00 cal ka BP (Fig. 5), potentially indicating an increase in anthropogenic effects on the landscape.

4.3.3. Core AM18-5

Barren: 4.90 to 4.77 cal ka BP (84-78 cm)

DAZ-1: 4.77 to 4.18 cal ka BP (78-67 cm)

DAZ-1 features two distinctive sections either side of the Late Chalcolithic – Philia Early Cypriot traditional archaeological interval boundary. Beginning with the lower section of DAZ-1, once again *Epithemia argus* dominates diatom assemblages, however decreases in abundance throughout the section, and combined with other diatom taxa (e.g. decreasing *Surirella crumena,* increased *Gomphonema minutum, Navicula oblonga,* and *Ulnaria vitrea*), suggests a shift from a mesotrophic to a more eutrophic setting (Fig. 6, Supplementary Figure S5). Fresh to fresh-brackish species dominate the assemblage in this zone, along with taxa indicating a pH neutral setting (Fig. 6). Decreasing water quality and oxygen saturation is suggested from the upper samples of this lower section at ca. 4.45 – 4.50 cal ka BP (Fig. 6).

In the upper section of DAZ-1 (the Philia Early Cypriot phase, ca. 4.45 - 4.30 cal ka BP) there is a recorded increase in higher salinity and eutrophic groups, alongside a continued decrease in the greater water quality taxa (Fig. 6). Furthermore, a combined decrease in *Surirella crumena* and *Epithemia argus* may suggest a restriction in moist subaerial habitats, while exclusively alkaliphilous and low nitrogen taxa suggest the onset of a more alkaline, nitrogen depleted environment (Fig. 6). At 4.30 cal ka BP continued oxygen depletion is suggested from diatom assemblages, and a decrease in *Navicula oblonga* combined with peak of *Nitzschia amphibia* may indicate an increase in anthropogenic impact (Fig. 6).

Barren: 4.18 to 3.99 cal ka BP (67-64 cm)

DAZ-2: 3.01 to 1.38 cal ka BP (49-18 cm)

A decreasing trend in *Navicula oblonga* from ca. 3.00 – 2.10 cal ka BP combined with the increase in both *Surirella ovalis* and *Campylodiscus hibernicus* from ca. 1.90 and ca. 1.50 cal ka BP respectively, may indicate an increasing human influence on the landscape throughout this

section. Decreasing trends in *Nitzschia amphibia, Diploneis ovalis* and *Gomphonema minutum* in coincidence with increasing *Epithemia argus* abundances from the base of the zone to ca. 1.90 cal ka BP may indicate increasing oxygen saturation and water quality through this section. Following ca. 1.90 cal ka BP these trends reverse to the top of the core, suggesting water quality decreases to the present day.

5. Discussion

5.1. Multiproxy history of the Akrotiri Marsh

Pollen and diatom proxy data from the Akrotiri Marsh are here combined to present a multiproxy history of the area, discuss palaeoclimatic events and their potential forcings (Fig. 7).

[Insert Figure 7]

5.1.1 Pre-4.50 cal ka BP

Pollen assemblages between ca. 4.60 – 4.50 cal ka BP indicate the dominance of wetland taxa, and taxa such as *Ipomoea* suggest the early establishment of a marsh environment (Tarasov et al., 1998; Gondelle, 2012; Gucel et al., 2013). *Cerealia*, while never abundant, features most prominently from 4.75 – 4.50 cal ka BP, indicating a potential agricultural signal from the surrounding landscape, which is supported by the cultivation weed taxa *Plantago,* and is consistent with a Late Chalcolithic subsistence economy that was more dependent on agriculture than hunting (Knapp, 2013). In the Hala Sultan Tekke record this interval is one of high and relatively stable growing season precipitation and temperature (Kaniewski et al., 2020). Diatom assemblages support the inference of marsh conditions between ca. 4.70 – 4.50 cal ka BP, recording gradually increasing salinity, eutrophication, and saprobity through time, likely driven by the seasonally fluctuating conditions. In summary, prior to ca. 4.50 cal ka BP multiple proxies suggest marsh conditions with seasonal fluctuations in water availability (Fig. 7).

5.1.2. The 4.2 ka BP Event

From ca. 4.50 cal ka BP both proxy datasets indicate decreasing water availability on the landscape and a more restricted marsh setting (Figs. 3, 4, 6), as well as the disappearance of evidence for agricultural activities (Figs. 3, 4). In the diatom data, this is indicated by taxa indicative of a more saline, alkaline, nutrient-enriched, phosphoric, anoxic, saprobic, and drier environment (Figs. 5, 6). The pollen data at this time records a decrease in wetland taxa, alongside the disappearance of *Cerealia* from all but one assemblage in core AM18-5 from 4.50 – 4.00 cal ka BP, and an increase in dry steppe and Mediterranean woodland taxa (Figs. 3, 4, S1, S2, S3). The peak in aridity, as defined from the pollen data, is between 4.50 and 4.35 ka cal BP. In the AM18-1 core this is seen as an expansion of dry steppe taxa at 4.35 ka cal BP and a second reduction in wetland vegetation at ca. 4.20 ka cal BP (Fig. 3). In the AM18-5 core the aridity event, as inferred from a reduction in wetland taxa, lasts from ca. 4.60 – 4.20 ka cal BP, whilst *Cerealia* is last present at ca. 4.30 ka cal BP (Fig. S3). Diatom datasets also indicate reduced anthropogenic impact on the surrounding landscape after 4.30 cal ka BP (Fig. 6). The records from Hala Sultan Tekke show a cooling trend starting at ca. 4.40 cal ka BP that reaches a maximum temperature anomaly of -2.7°C, whilst winter rainfall is reconstructed to have reduced by 41 mm between 4.35 – 4.20 cal ka BP (Kaniewski et al., 2020). The interval of aridity is reconstructed as starting slightly earlier at the Akrotiri Marsh, peak aridity is consistent with a short dry interval recorded from the Sea of Galilee at ca. 4.30 cal ka BP (Langgut et al., 2016) and the onset of the 4.2 ka BP event at Hala Sultan Tekke (Kaniewski et al., 2020).

5.1.3. The 3.2 ka BP Event

The 3.2 ka BP Event is seen in the pollen record from the Akrotiri Marsh by a minimum in wetland vegetation at 3.17 cal ka BP followed by a peak in wetland taxa between 3.10 – 2.97 cal ka BP and finally a peak in dry steppe taxa at 2.80 cal ka BP (Fig. 3). The diatom data from the Akrotiri Marsh also suggest a period of aridity from 3.21-3.13 cal ka BP and the potential for reduced human impacts on the environment (Fig. 5). At Hala Sultan Tekke, peak aridity is centred on 3.15 cal ka BP when winter rainfall decreased by 30 mm and at 2.90/2.85 cal ka BP with a decrease in winter rainfall of 8 mm (Kaniewski et al., 2020). Spring rainfall also decreases in the Hala Sultan Tekke record, with the greatest minima recorded throughout the Bronze Age (Kaniewski et al., 2020). A return to more normal winter and spring rainfall is reconstructed in the humid interval at 3.00-2.95 cal ka BP (Kaniewski et al., 2019, 2020). Our new results are in agreement with this, showing the minimum in wetland vegetation during the first and driest peak of the 3.2 cal ka BP event and a turnover from Cupressaceae to *Pinus* and an increase in Urticaceae, which together could show a decrease in agricultural activity and abandonment of lower elevation sites (Bottema, 1982; Gucel et

al., 2013). Whilst the second aridity peak recorded at Hala Sultan Tekke is much less extreme, taking into account the full range of uncertainty, the drop during the second 3.2 cal ka BP arid peak was 2 – 17 mm in the winter and 2.6 – 9.3 mm in spring (Kaniewski et al., 2020). This more muted precipitation event is less pronounced in the Akrotiri Marsh record, indicated by a peak in dry steppe taxa at ca. 2.8 ka cal BP (Fig. 3). At ca. 3.15 cal ka BP, archaeological records display the widespread voluntary abandonment of both coastal centres, such as Hala Sultan Tekke, Ayios Dhimitrios, Alassa, Maroni, Morphou *Toumba tou Skourou*, Maa *Palaeokastro* and Pyla *Kokkinokremnos* (Brown, 2013; Kaniewski et al., 2013, 2019; Knapp and Manning, 2016), and inland settlements specialising in agriculture, mining and pottery production, such as Myrtou *Pigadhes*, Athienou Bamboulari tis Koukounninas, and Apliki *Karamallos* (Knapp and Manning, 2016). Destruction of monumental structures and abandonment of town centres is also present at some of the largest societal structures on the island, including the nearest to the Akrotiri Marsh site Alassa *Paleotaverna* (Knapp and Manning, 2016). The abandonment of Alassa *Paleotaverna* further up the Kouris River catchment occurred before the second aridity peak of the 3.2 cal ka BP event (using dates provided in Knapp, 2013). Based on the extreme decline in rainfall recorded in the Akrotiri Marsh, which has a hydrology part-controlled by the Kouris River catchment, and supported by the reconstructions from distal Hala Sultan Tekke could indicate this agricultural centre was a victim of the first cold-arid peak of the 3.2 cal ka BP event.

Preceding the main 3.2 ka BP Event, there is evidence for increasing aridity in the Akrotiri Marsh as there are in many other Mediterranean records (Kaniewski et al., 2010, 2013, 2019; Bernhardt et al., 2012; Drake, 2012; Langgut et al., 2016). Diatom assemblages record an increase in salinity, alkalinity and nutrient enrichment between ca. 3.70 – 3.40 cal ka BP, along with a decrease in oxygen saturation and subaerial moist habitats (Fig. 5). Pollen assemblages record a peak in dry steppe taxa from ca. 3.40 – 3.35 cal ka BP (Fig. 3). Combined, these proxy records indicate a reduction in water availability during this interval (Fig. 7). This is coincident with a pan-Mediterranean wide centennial-scale cold and arid climate event that occurred between 3.50 – 3.30 cal ka BP (Finné et al., 2019). By contrast, at Hala Sultan Tekke this time interval is shown to have mostly warmer temperature anomalies and only a minor decrease in winter rainfall (Kaniewski et al., 2020). Following this, both proxy records from the Akrotiri Marsh suggest a short interval of increased water availability centred on ca. 3.35 cal ka BP (Figs. 3, 5) that is coincident with the Late Bronze Age peak in spring precipitation and a brief warming in an otherwise cooling trend reported from the Hala Sultan Tekke (Kaniewski et al., 2020), before water availability continues to decrease into the 3.2 ka BP event (Fig. 7). The pollen record at this

time shows strong fluctuations between wetland, Mediterranean woodland and steppe taxa, suggesting a period of variable precipitation (Fig. 3). Cyprus is latitudinally parallel with the Northern Levant mainland, where it has been previously established that the onset of 3.2 ka BP Event began earlier (ca. 3.45 cal ka BP) (Kaniewski et al., 2008; Sorrel and Mathis, 2016) than in the southern Levant (ca. 3.25 cal ka BP) (Schilman et al., 2002; Litt et al., 2012). Results from the Akrotiri Marsh indicate that this earlier onset time for the 3.2 ka BP Event in the northern Levant is also consistent for Cyprus, where pollen assemblages in core AM18-1 record increased aridity events from ca. 3.40 cal ka BP. This is however, not recorded in the eastern Larnaca Salt Lake region (Kaniewski et al., 2013, 2019, 2020).

5.1.4. Post-3.2 ka BP event

Following the second aridity peak at ca. 2.80 ka cal BP, there is a trend towards increased water availability in both the pollen and diatom records (Fig. 7). This is accompanied by a renewed signal for agricultural activity in the area, which is consistent with the pattern seen at Hala Sultan Tekke (Kaniewski et al., 2020). In the pollen records the increasing humidity trend reaches a peak in fen trees and riverine forest at around 2.60 cal ka BP and a minimum in the dry steppe vegetation at 2.40 cal ka BP (Figs. 3, 4). Diatom assemblages between ca. 3.10 – 2.10 cal ka BP suggest decreasing salinity and phosphorus concentrations, along with increasing oxygen concentration and anthropogenic influence (Figs. 5,6). In the Hala Sultan Tekke record this is an interval of above average winter rainfall and a peak in spring rainfall (Kaniewski et al., 2020). The increase of Mediterranean woodland and dry steppe vegetation at ca. 2.30 ka cal BP in core AM18-5 could relate to the below average spring rainfall and declining winter rainfall reported from the Hala Sultan Tekke record (Kaniewski et al., 2020). In AM18-1, the increase in wetland pollen taxa from ca. 1.90 – 1.55 cal ka BP is coincident with the highest winter and spring rainfall recorded in the Hala Sultan Tekke record (Kaniewski et al., 2020). At ca. 1.50 cal ka BP the sedimentology, pollen and diatom assemblages all change in the Akrotiri Marsh suggesting a major change in the local environment (Figs. 2, 3, 5). The reconstructions from near Hala Sultan Tekke show this is a period of cold-wet winters linked with a Late Antique cold interval (Kaniewski et al., 2020). It is also when a series of earthquakes affected the region with destruction at the nearby settlement of Kourion and the harbour at Dreamers Bay (James et al., 2021). Disentangling the relative roles of cold-wet winters and earthquakes on the development of the Akrotiri Marsh is beyond the scope of this paper. Diatom assemblages continue to record decreasing salinity and increasing oxygen concentration from ca. 1.80 – 1.38 cal ka BP, after which the marsh becomes

more saline once more (Fig. 5). From Hala Sultan Tekke, the period 1.00 – 0.50 cal ka BP is one of above average winter precipitation (Kaniewski et al., 2020) and corresponds to increased amounts of wetland plant pollen in the Akrotiri Marsh record (Fig. 3).

5.2. Palaeoclimatology of the Akrotiri Marsh

At the Akrotiri Marsh there is a clear correlation between the onset of lesser water availability inferred by pollen and diatom assemblages (Fig. 7, zone 1b in each proxy), and the North Atlantic Oscillation (NAO) inversion to a more positive state at ca. 4.45 cal ka BP (Fig. 7) (Olsen et al., 2012; Margaritelli et al., 2016). This turnover also occurs towards the end of an interval of increased Siberian High intensity, between 4.60 and 4.45 cal ka BP (Fig. 7) (Rohling et al., 2002; Mayewski et al., 2004). The following interval of increased Siberian High intensity between ca. 3.80 – 3.60 cal ka BP does not appear to correlate with any arid climate inferences from the Akrotiri Marsh proxy records. However, the onset of consistently positive NAO conditions from ca. 3.35 – 3.10 cal ka BP does correlate with a series of aridity peaks in pollen and diatom records (Fig. 7, AM18-1 zone 2 in each proxy), as well as an interval of increased Siberian High intensity between 3.40 – 3.00 cal ka BP (Rohling et al., 2002; Mayewski et al., 2004).

It appears therefore, that climate fluctuations at the Akrotiri Marsh, Cyprus, most closely correlate to the configuration of the NAO, and to a lesser extent the intensity of the Siberian High pressure system. It has been previously documented that the Siberian High anticyclone likely has a direct impact on modern monthly precipitation on Cyprus (Lingis and Michaelides, 2009), and that shifts in the Siberian High intensity have potentially induced large-scale climatic fluctuations in the at ca. 3.00 cal ka BP (Geraga et al., 2010). There is evidence that the NAO is connected to millenia-scale shifts in sea surface temperatures and climates in the eastern Mediterranean and Middle East (Rimbu et al., 2003; Wanner et al., 2008), as well as having been connected to increasing aridity in East Africa from ca. 3.50 cal ka BP (Kaniewski et al., 2015), and associated with Late Bronze Age droughts in the Aegean, eastern Mediterranean, and west Asia (Kaniewski et al., 2015). By better understanding the Holocene palaeoenvironments of Cyprus, we may better understand the distribution and expression of the dominant global climate forcing mechanisms in the eastern Mediterranean, particularly in relation to the lesser explored effects of the NAO in this region.

5.3. “Societal Collapse” or more nuanced societal changes linked to climate?

A number of authors have suggested an environmental cause to the Late Bronze Age Collapse (Alpert et al., 1989; Bryson et al., 1974; Butzer & Harris, 2007; Carpenter, 1966; Dalfes et al., 1997; Neumann et al., 1987; Weiss, 1982, 1997), however the role of climate change in eastern Mediterranean Bronze Age societal shifts is often subject to lively debate (Cline, 2014; Knapp and Manning, 2016; Schloen, 2017). One causal hypothesis is that climate change directly and primarily determined land cover and vegetation throughout the Mediterranean and thus provided the limitations for Bronze Age societies that, driven by necessity, would have predictable responses in order to fully adapt to climatic changes (Jalut et al., 2009; Di Rita et al., 2018). It is also hypothesised that climate change had a more direct impact on human society and populations through multiple pathways as well as through vegetation turnover, resulting in political and economic turmoil and migrations that then had a further direct effect on land cover (Rosen, 2007; Kaniewski and Van Campo, 2017). Lastly, there is a purely human hypothesis, that populations alone caused the observed changes in land cover and vegetation irrespective of climate influence (Hughes, 2014). A recent synthesis on pollen and archaeo-demographic archives suggests that during the Bronze Age (prior to ca. 3.00 ka BP), a combination of hypothesis one (climate affecting vegetation and human societies directly) and hypothesis two (purely anthropogenically induced vegetation alteration) were the main factors in changing landscapes (Roberts et al., 2019). Throughout the Mediterranean Bronze Age, long-term and medium-term climatic adversity has often destabilised civilisations through multiple pathways, whereas societies have often learnt to cope with recurring shorter-term climatic cycles (McMichael, 2012). There is also evidence that populations expanded not only in spite of long-term climatic shifts, but also due to them, with climatic adversity acting as a stimulus rather than a hindrance to adequately structured societal/organisational adaptive strategies (Roberts et al., 2019). While numerous proxy datasets suggest more arid conditions, societal set-up and human responses were a key factor (Holmgren et al., 2016; Knapp and Manning, 2016), and when considering agricultural shifts, single causes should be avoided and integrated environmental, economic, and social factors must be formed into a causal chain (Riehl et al., 2012).

The climatic inferences documented in this paper are congruent with, and build upon, other climate research from Cyprus during the Bronze Age interval, and we can begin to see a consistent and widespread climate reconstruction throughout the southern margins of the island. While Figure 7 certainly displays a co-incidence of climatic and societal shifts on Cyprus, it is important to note that it is beyond the scope of this paper - that is, to provide a contextual climatic reconstruction for archaeological research on the island and other research in these fields - to

conclude at this stage whether the documented climate shifts acted as contributors, instigators or exacerbators in societal shifts during the Cypriot Bronze Age. This question would likely benefit from the introduction of more proxy analyses at previously studied sites, such as geochemical analyses that could give insight to fluctuations in the mining and metal economies on Cyprus during the Bronze Age.

6. Conclusions

Pollen and diatom assemblages from the Akrotiri Marsh provide a consistent and detailed record of environmental change on Cyprus during the late Holocene. Two sediment cores featuring average chronological resolutions of one date per 1000 years, potentially allow for inferring that both the 4.2 ka BP and 3.2 ka BP climate events had an impact on the island's water balance. Increasing aridity speculated to occur from 4.50 cal ka BP is shown by increasing Mediterranean woodland and dry steppe pollen types, whilst the diatom assemblage indicates gradually increasing salinity, eutrophication and saprobity at the Akrotiri Marsh, while oxygen saturation gradually decreased. Both proxies indicate maximum aridity potentially during the 4.2 ka BP event. The inferred 3.2 ka BP event in the pollen record is identified as an initial increase in aridity, followed by a brief interval of humidity, and then a second interval of increased aridity. This is very similar to the nature and timing of the "W-shaped" signal identified at the nearby site of Pyla *Kokkinokremno* (Kaniewski et al., 2019; 2020). These results also occur in close correlation with shifts in the NAO cycle, and Late Bronze Age reconstructions are coincident with the widespread abandonment of many coastal archaeological sites and inland urban centres on Cyprus. Our new record from the Akrotiri Marsh shows that a climatic influence on societal change cannot be dismissed at this site.

Acknowledgements

We are immensely grateful to Chris Hadjigeorgiou of the Geological Survey Department, Cyprus, Pantelis Charilaou of the Sovereign Base Area Administration Environmental Department, Thomas Hadjikyriakou of the Akrotiri Environmental Education and Information Centre, the Ministry of Defence and Defence Infrastructure Organisation for enabling us to undertake fieldwork and take samples. The fieldwork was kindly

supported by a grant from the Council for British Research in the Levant and CJH thanks Northumbria University for funding his PhD. Lesley Dunlop, Dave Thomas and Will Thomas are thanked for their kind assistance in the lab.

7. References

Allen, M., Scaife, R., Manning, A., Edwards, R., 2009. The development and vegetation history of the Akrotiri salt lake, Cyprus. Quat. Newsl. 119, 1–16.

Alpert, P., Jacobeit, S., Fernandez, J., Gonzalez-Rouco, F., Garcia-Herrera, R., Rodo, X., Brunetti, M., Nanni, T., Maugeri, M., Turkes, M., Gimeno, L., Ribera, P., Brunet, M., Trigo, I., Crepon, M., Mariotti, A., 2006. Relations between variability in the Mediterranean region and Mid-latitude variability, in: Lionello, P., Malanotte-Rizzoli, P., Boscolo, R. (Eds.), The Mediterranean Climate: An Overview of the Main Characteristics and Issues. Elsevier.

Alpert, P., Neumann, J., 1989. An Ancient "Correlation" between Streamflow and Distant Rainfall in the near East. J. Near East. Stud. 48, 313–314.

Álvarez-Blanco, I., Blanco, S., 2014. Benthic diatoms from Mediterranean coasts. Acta Botanica Hungarica 56.

Bahls, L., Boynton, B., Johnston, B., 2018. Atlas of diatoms (Bacillariophyta) from diverse habitats in remote regions of western Canada. PhytoKeys 105, 1–186. https://doi.org/10.3897/phytokeys.105.23806

Baioumy, H., Kayanne, H., Tada, R., 2010. Reconstruction of lake-level and climate changes in Lake Qarun, Egypt, during the last 7000 years. J. Great Lakes Res. 36, 318–327. https://doi.org/10.1016/j.jglr.2010.03.004

Battarbee, R., 1986. Diatom analysis, in: Berglund, B. (Ed.), Handbook of Holocene Palaeoecology and Palaeohydrology. John Wiley: Chichester, pp. 527–557.

Battarbee, R., Carvalho, L., Jones, V., Flower, R., Cameron, N., Bennion, H., Juggins, S., 2001. Diatoms, in: Smol, J., Birks, H., Last, W.

(Eds.), Tracking Environmental Change Using Lake Sediments. Volume 3: Terrestrial, Algal, and Siliceous Indicators. Kluwer: Dordrecht, pp. 155–202.

Battarbee, R., Juggins, S., Gasse, F., Anderson, N., Bennion, H., Cameron, N., 1998. European Diatom Database (EDDI): an information system for palaeoenvironmental reconstruction, European Climate Science Conference, Vienna City Hall, Vienna.

Bernhardt, C., Horton, B., Stanley, J., 2012. Nile Delta vegetation response to Holocene climate variability. Geology 40, 615–618. https://doi.org/10.1130/G33012.1

Bini, M., Zanchetta, G., Persoiu, A., Cartier, R., Català, A., Cacho, I., Dean, J., Di Rita, F., Drysdale, R., Finne, M., Isola, I., Jalalia, B., Lirer, F., Magri, D., Masi, A., Marks, L., Mercuri, A., Peyron, O., Sadori, L., Sicre, M.A., Welc, F., Zielhofer, C., Brisset, E., 2019. The 4.2 ka BP Event in the Mediterranean region: an overview. Clim. Past 15, 555–577

Birol, E., Koundouri, P., Koundouris, Y., 2011. Water Resources Management and Wetland Conservation: The Case of Akrotiri Wetland in Cyprus., in: Koundouri, P. (Ed.), Water Resources Allocation. Global Issues in Water Policy. Springer, Dordrecht.

Blaauw, M., Christen, J., 2019. rBacon Bayesian Age-Depth Modelling Approach 2.3.2. R Packag.

Blanco, S., 2016. Aqualitas-retos Identificación y Clasificación Automática de Diatomeas [WWW Document]. Imarenabio, Spain. URL http://aqualitas-retos.es/species/

Bond, G., 1997. A Pervasive Millennial-Scale Cycle in North Atlantic Holocene and Glacial Climates. Science (80-.). 278, 1257–1266. https://doi.org/10.1126/science.278.5341.1257

Bond, G., Kromer, B., Beer, J., Muscheler, R., Evans, M., Showers, W., Hoffmann, S., Lotti-bond, R., Hajdas, I., Bonani, G., 2001. Persistent Solar Influence on North Atlantic Climate During the Holocene. Science (80-.). 294, 2130–2136. https://doi.org/10.1126/science.1065680

Bottema, S., 1982. Palynological Investigations in Greece with Special Reference to Pollen as an Indicator of Human Activity. Palaeohistoria 24, 257–289.

Bottema, S., 1976. Note on Pollen, in: Åström, P. (Ed.), Hala Sultan Tekke 1 (Vol. 95). Paul Åströms Förlag: Studies in Mediterranean

Archaeology, Jonsered.

Bottema, S., 1966. Palynological Investigation of a Settlement near Kalopsidha, in: Åström, P. (Ed.), Excavations at Kalopsidha and Ayios Iakovos in Cyprus. Paul Åströms Förlag: Studies in Mediterranean Archaeology, Lund, pp. 133–134.

Bouchal, J., Mayda, S., Zetter, R., Grímsson, F., Akgün, F., Denk, T., 2017. Miocene palynofloras of the Tınaz lignite mine, Muğla, southwest Anatolia: Taxonomy, palaeoecology and local vegetation change. Rev. Palaeobot. Palynol. 243, 1–36. https://doi.org/10.1016/j.revpalbo.2017.02.010

Bouchal, J., Zetter, R., Denk, T., 2016. A combined light and scanning electron microscopy study. Grana 55, 179–245. https://doi.org/10.1080/00173134.2015.1108362

Brown, M., 2013. Waterways and the Political Geography of South-East Cyprus in the Second Millennium BC. Annu. Br. Sch. Athens 108, 121–136. https://doi.org/10.1017/S006824541300004X

Brullo, S., Giusso del Galdo, G., Guarino, R., 2005. The orophilous dwarf-shrub vegetation of Mt. Troodos (Cyprus). Bot. Chron. 18, 63–73.

Bryce, T., 2005. The Kingdom of the Hittites. Oxford University Press.

Bryson, R., Lamb, H., Donley, D., 1974. Drought and the Decline of Mycenae. Antiquity 48, 46–50.

Butzer, K., Harris, S., 2007. Geoarchaeological approaches to the environmental history of Cyprus: explication and critical evaluation. J. Archaeol. Sci. 34, 1932–1952.

Cantonati, M., Angeli, N., Spitale, D., Lange-Bertalot, H., 2016. A new Navicula (Bacillariophyta) species from low-elevation carbonate springs affected by anthropogenic disturbance. Fottea 16, 255–265. https://doi.org/10.5507/fot.2016.013

Cantonati, M., Lange-Bertalot, H., Kelly, M., Angeli, N., 2018. Taxonomic and ecological characterization of two ulnaria species (Bacillariophyta) from streams in Cyprus. Phytotaxa 346, 78–92. https://doi.org/10.11646/phytotaxa.346.1.4

Carpenter, R., 1966. Discontinuity in Greek Civilization. Cambridge University Press.

Catling, H., 1975. Cyprus in the Late Bronze Age. Cambridge Anc. Hist. 2.

Chester, P., Raine, J., 2001. Pollen and spore keys for Quaternary deposits in the northern Pindos Mountains, Greece, Grana. https://doi.org/10.1080/00173130152987535

Cline, E., 2014. 1177 B.C.: The Year Civilization Collapsed. Princeton University Press.

Cohen, Y., Singer, I., 2006. Late Synchronism between Ugarit and Emar, in: Amit, Y., Zvi, E., Finkelstein, I., Lipschits, O. (Eds.), Essays on Ancient Israel in Its Near Eastern Context. A Tribute to Nadav Na'ama. Winona Lake: Eisenbrauns, pp. 123–139. https://doi.org/10.1038/srep29623

Cooper, E., 1997. The Middle Bronze Age of the Euphrates Valley, Syria: Chronology, regional interaction and cultural exchange. Dep. Near Middle East. Civilizations Ph.D., 400.

Cugny, C., Mazier, F., Galop, D., 2010. Modern and fossil non-pollen palynomorphs from the Basque mountains (western Pyrenees, France): The use of coprophilous fungi to reconstruct pastoral activity. Veg. Hist. Archaeobot. 19, 391–408. https://doi.org/10.1007/s00334-010-0242-6

Cullen, H., DeMenocal, P., 2000. North Atlantic influence on Tigris-Euphrates streamflow. Int. J. Climatol. 20, 853–863. https://doi.org/10.1002/1097-0088(20000630)20:8<853::AID-JOC497>3.0.CO;2-M

Dalfes, H., Nüzhet, G., Weiss, H., 1997. Third Millennium BC Climate Change and Old World Collapse. Springer.

Davies, S., Jackson, S., 2006. The biological condition gradient: A descriptive model for interpreting change in aquatic ecosystems. Ecol. Appl. 16, 1251–1266. https://doi.org/10.1890/1051-0761(2006)016[1251:TBCGAD]2.0.CO;2

Davis, B., Brewer, S., 2009. Orbital forcing and role of the latitudinal insolation/temperature gradient. Clim. Dyn. 32, 143–165. https://doi.org/10.1007/s00382-008-0480-9

Delgado, C., Ector, L., Novais, M., Blanco, S., Hoffmann, L., Pardo, I., 2013. Epilithic diatoms of springs and spring-fed streams in Majorca Island (Spain) with the description of a new diatom species Cymbopleura margalefii sp. nov. Fottea 13, 87–104.

https://doi.org/10.5507/fot.2013.009

Delipetrou, P., Makhzoumi, J., Dimopoulos, P., Georghiou, K., 2008. Cyprus, in: Vogiatzakis, I., Pungetti, G., Mannion, A. (Eds.), Mediterranean Island Landscapes: Natural and Cultural Approaches. Springer, pp. 170–203.

Demske, D., Tarasov, P., Nakagawa, T., 2013. Atlas of pollen, spores and further non-pollen palynomorphs recorded in the glacial-interglacial late Quaternary sediments of Lake Suigetsu, central Japan. Quat. Int. 290–291, 164–238. https://doi.org/10.1016/j.quaint.2012.02.002

Desprat, S., Combourieu-Nebout, N., Essallami, L., Sicre, M.A., Dormoy, I., Peyron, O., Siani, G., Bout Roumazeilles, V., Turon, J.L., 2013. Deglacial and holocene vegetation and climatic changes in the southern central Mediterranean from a direct land-sea correlation. Clim. Past 9, 767–787. https://doi.org/10.5194/cp-9-767-2013

Di Rita, F., Lirer, F., Bonomo, S., Cascella, A., Ferraro, L., Florindo, F., Insinga, D., Lurcock, P., Margaritelli, G., Petrosino, P., Rettori, R., Vallefuoco, M., Magri, D., 2018. Late Holocene forest dynamics in the Gulf of Gaeta (central Mediterranean) in relation to NAO variability and human impact. Quat. Sci. Rev. 179, 137–152. https://doi.org/10.1016/j.quascirev.2017.11.012

Di Rita, F., Magri, D., 2019. The 4.2 ka event in the vegetation record of the central Mediterranean. Clim. Past 15, 237–251. https://doi.org/10.5194/cp-15-237-2019

Diatoms of North America [WWW Document], 2017. . Source diatom Identif. Ecol. URL https://diatoms.org

Drake, B., 2012. The influence of climatic change on the Late Bronze Age Collapse and the Greek Dark Ages. J. Archaeol. Sci. 39, 1862–1870. https://doi.org/10.1016/j.jas.2012.01.029

Dreal center-Val de Loire, Regional Directorate for the Environment, Planning and Housing [WWW Document], 2019. . Ministère la Transit. écologique Solidaire. URL http://www.centre-val-de-loire.developpement-durable.gouv.fr/

El-Amier, Y., 2015. Morphological studies of the pollen grains for some hydrophytes in coastal Mediterranean lakes, Egypt. Egypt. J. Basic Appl. Sci. 2, 132–138. https://doi.org/10.1016/j.ejbas.2015.04.001

Fahmi, A., Susilawati, A., Sarwani, M., 2021. The role of peat decomposition stage on iron solubility and distribution in tidal swamps. IOP Conf.

Ser. Earth Environ. Sci. 648. https://doi.org/10.1088/1755-1315/648/1/012174

Fall, P., 2012. Modern vegetation, pollen and climate relationships on the Mediterranean island of Cyprus. Rev. Palaeobot. Palynol. 185, 79–92. https://doi.org/10.1016/j.revpalbo.2012.08.002

Finné, M., Woodbridge, J., Labuhn, I., Roberts, N., 2019. Holocene hydro-climatic variability in the Mediterranean: A synthetic multi-proxy reconstruction. The Holocene 29, 42.

Gelorini, V., Verbeken, A., van Geel, B., Cocquyt, C., Verschuren, D., 2011. Modern non-pollen palynomorphs from East African lake sediments. Rev. Palaeobot. Palynol. 164, 143–173. https://doi.org/10.1016/j.revpalbo.2010.12.002

Geraga, M., Ioakim, C., Lykousis, V., Tsaila-Monopolis, S., Mylona, G., 2010. The high resolution palaeoclimatic and palaeoceanographic history of the last 24,000 years in the central Aegean Sea, Greece. Palaeogeogr. Palaeoclimatol. Palaeoecol. 287, 101–115. https://doi.org/10.1016/j.palaeo.2010.01.023

Ghilardi, M., Cordier, S., Carozza, J., Psomiadis, D., Guilaine, J., Zoumeni, Z., Demory, F., Delanghe-Sabatier, D., Vella, M., Bony, G., Morhange, C., 2015. The holocene fluvial history of the tremithos river (South central cyprus) and its linkage to archaeological records. Environ. Archaeol. 20, 184–201. https://doi.org/10.1179/1749631414Y.0000000057

Gondelle, J., 2012. Akrotiri Peninsula Environmental Management Plan - Final Report. Sover. Base Areas Adm. 303.

Grimm, E., 2011. TILIA software. Illinois State Museum Res. Collect. Cent.

Grimm, E., 1987. CONISS: a FORTRAN 77 program for stratigraphically constrained cluster analysis by the method of incremental sum of squares. Comput. Geosci. 13, 13–35. https://doi.org/10.1016/0098-3004(87)90022-7

Gucel, S., Guvensen, A., Ozturk, M., Celik, A., 2013. Analysis of airborne pollen fall in Nicosia (Cyprus). Environ. Monit. Assess. 185, 157–169. https://doi.org/10.1007/s10661-012-2540-1

Gucel, S., Kadis, C., Ozden, O., Charalambidou, I., Linstead, C., Fuller, Kounnamas, C., Ozturk, M., 2012. Assessment of biodiversity differences between natural and artificial Wetlands in Cyprus. Pakistan J. Bot. 44, 213–224.

Guiry, M., Guiry, G., 2020. AlgaeBase [WWW Document]. World-wide Electron. Publ. Natl. Univ. Ireland, Galway. URL https://www.algaebase.org

Hadjichambis, A., Della, A., Paraskeva-Hadjichambi, D., 2004. Flora of the sand dune ecosystems of Cyprus. Proc. 10th MEDECOS Conf. 1–7.

Höflmayer, F., 2017. The Late Third Millennium B.C. in the Ancient Near East and Eastern Mediterranean: A Time of Collapse and Transformation, in: Höflmayer, F. (Ed.), The Late Third Millennium in the Ancient Near East. Chronology, C14 and Climate Change. The Oriental Institute of the University of Chicago, pp. 1–28.

Holmgren, K., Gogou, A., Izdebski, A., Luterbacher, J., Sicre, M., Xoplaki, E., 2016. Mediterranean Holocene climate, environment and human societies. Quat. Sci. Rev. 136, 1–4. https://doi.org/10.1016/j.quascirev.2015.12.014

Hughes, J., 2014. Environmental Problems of the Greeks and Romans: Ecology in the Ancient Mediterranean, 2nd Editio. ed. Johns Hopkins University Press.

iNaturalist Diatom Database [WWW Document], 2013. . Calif. Acad. Sci. URL https://www.inaturalist.org/taxa/123880-Bacillariophyceae

Isola, I., Zanchetta, G., Drysdale, R., Regattieri, E., Bini, M., Bajo, P., Hellstrom, J., Baneschi, I., Lionello, P., Woodhead, J., Greig, A., 2019. The 4.2 ka BP event in the central Mediterranean: new data from Corchia speleothems (Apuan Alps, central Italy). Clim. Past 15, 135–151. https://doi.org/10.5194/cp-2018-127

Jalut, G., Dedoubat, J., Fontugne, M., Otto, T., 2009. Holocene circum-Mediterranean vegetation changes: Climate forcing and human impact. Quat. Int. 200, 4–18. https://doi.org/10.1016/j.quaint.2008.03.012

James, S., Blue, L., Rogers, A., Score, V., 2021. From phantom town to maritime cultural landscape and beyond: Dreamer's Bay Roman-Byzantine 'port', the Akrotiri Peninsula, Cyprus, and eastern Mediterranean maritime communications. Levant 1–24.

Jeux de donnees de reference, Sandre Service s'administration nationale des donnees et rederentiels sur l'eau [WWW Document], 2017. . Off. Int. l'Eau. URL http://id.eaufrance.fr/apt/12594

Juggins, S., 2001. The European Diatom Database User Guide.

Jüttner, I., Bennion, H., Carter, C., Cox, E., Ector, L., Flower, R., Jones, V., Kelly, M., Mann, D., Sayer, C., Turner, J., Williams, D., 2017. Freshwater Diatom Flora of Britain and Ireland [WWW Document]. Amgueddfa Cymru - Natl. Museum Wales. URL https://naturalhistory.museumwales.ac.uk/diatoms/Home.php

Kaniewski, D., Guiot, J., Van Campo, E., 2015. Drought and societal collapse 3200 years ago in the Eastern Mediterranean: A review. Wiley Interdiscip. Rev. Clim. Chang. 6, 369–382. https://doi.org/10.1002/wcc.345

Kaniewski, D., Marriner, N., Bretschneider, J., Jans, G., Morhange, C., Cheddadi, R., Otto, T., Luce, F., Van Campo, E., 2019. 300-year drought frames Late Bronze Age to Early Iron Age transition in the Near East: new palaeoecological data from Cyprus and Syria. Reg. Environ. Chang. 19, 2287–2297. https://doi.org/10.1007/s10113-018-01460-w

Kaniewski, D., Marriner, N., Cheddadi, R., Fischer, P., Otto, T., Luce, F., Van Campo, E., 2020. Climate Change and Social Unrest: A 6,000-Year Chronicle From the Eastern Mediterranean. Geophys. Res. Lett. 47, https://doi.org/10.1029/2020gl087496

Kaniewski, D., Paulissen, E., Van Campo, E., Al-Maqdissi, M., Bretschneider, J., Van Lerberghe, K., 2008. Middle East coastal ecosystem response to middle-to-late Holocene abrupt climate changes. Proc. Natl. Acad. Sci. U. S. A. 105, 13941–13946. https://doi.org/10.1073/pnas.0803533105

Kaniewski, D., Paulissen, E., Van Campo, E., Weiss, H., Otto, T., Bretschneider, J., Van Lerberghe, K., 2010. Late second-early first millennium BC abrupt climate changes in coastal Syria and their possible significance for the history of the Eastern Mediterranean. Quat. Res. 74, 207–215. https://doi.org/10.1016/j.yqres.2010.07.010

Kaniewski, D., Van Campo, E., 2017. The 3.2 kyr BP event and the Late Bronze age crisis, a climate-induced spiral of decline, in: Weiss, H. (Ed.), Megadrought and Collapse: From Early Agriculture to Angkor. Oxford University Press, pp. 161–182.

Kaniewski, D., Van Campo, E., Guiot, J., Le Burel, S., Otto, T., Baeteman, C., 2013. Environmental Roots of the Late Bronze Age Crisis. PLoS One 8, 1–10. https://doi.org/10.1371/journal.pone.0071004

Kassinis, N., Charalambidou, I., 2021. Autumn migration of the Red-footed Falcon, Falco vespertinus, at Akrotiri Peninsula, Cyprus 2009-2019

(Aves: Falconiformes). Zool. Middle East 67, 19–24.

Katrantsiotis, C., Norström, E., Smittenberg, R., Finne, M., Weiberg, E., Hättestrand, M., Avramidis, P., Wastegård, S., 2019. Climate changes in the Eastern Mediterranean over the last 5000 years and their links to the high-latitude atmospheric patterns and Asian monsoons. Glob. Planet. Change 175, 36–51. https://doi.org/10.1016/j.gloplacha.2019.02.001

Kearns, C., Manning, S., 2019. New Directions in Cypriot Archaeology. Cornell University Press.

Kelly, M., Gómez-Rodríguez, C., Kahlert, M., Almeida, S., Bennett, C., Bottin, M., Delmas, F., Desrey, J., Dörflinger, G., Kennedy, B., Marvan, P., Opatrilova, L., Pardo, I., Pfister, P., Rosebery, J., Schneider, S., Vilbaste, S., 2012. Establishing expectations for pan-European diatom based ecological status assessments. Ecol. Indic. 20, 177–186. https://doi.org/10.1016/j.ecolind.2012.02.020

Kennedy, M., 2016. The End of the 3rd Millennium BC in the Levant: New Perspectives and Old Ideas. Levant 48, 1–32. https://doi.org/10.1080/00758914.2016.1143750

Knapp, A., 2013. The archaeology of Cyprus: from earliest prehistory through the Bronze Age. Cambridge University Press.

Knapp, A., 2011. The Archaeology of Late Bronze Age Cypriot Society: The Study of Settlement, Survey and Landscape, in: Occasional Papers, Department of ArchaeologyUniversity of Glasgow.

Knapp, A., 2008. Prehistoric & Protohistoric Cyprus. Oxford University Press.

Knapp, A., Manning, S., 2016. Crisis in Context: The End of the Late Bronze Age in the Eastern Mediterranean. Am. J. Archaeol. 120, 99. https://doi.org/10.3764/aja.120.1.0099

Krammer, K., Lange-Bertalot, H., 1991. Bacillariophyceae 4. Teil: Achnanthaceae, Kritische Ergänzungen zu Navicula (Lineolatae) und Gomphonema, Gesamtliteraturverzeichnis, in: Ettl, H., Gärtner, G., Gerloff, J., Heynig, H., Mollenhauer, D. (Eds.), Süsswasser Flora von Mitteleuropa. p. 437.

Krammer, K., Lange-Bertalot, H., 1986. Bacillariophyceae 1. Teil: Naviculaceae, in: Ettl, H., Gerloff, J., Heynig, H., Mollenhauer, D. (Eds.), Süsswasser Flora von Mitteleuropa. p. 876.

Lange-Bertalot, H., 2001. Diatoms of Europe. A.R.G. Ganter Verlag K.G.

Lange-Bertalot, H., Metzeltin, D., 1996. Indicators of oligotrophy - 800 taxa representative of three ecologically distinct lake types, Carbonate buffered - Oligodystrophic - Weakly buffered soft water, in: Lange-Bertalot, H. (Ed.), Iconographia Diatomologica. Annotated Diatom Micrographs. Vol. 2. Ecology, Diversity, Taxonomy. Koeltz Scientific Books. Königstein, Germany, p. 390.

Langgut, D., Adams, M., Finkelstein, I., 2016. Climate, settlement patterns and olive horticulture in the southern Levant during the Early Bronze and Intermediate Bronze Ages (c. 3600 – 1950 BC). Levant 48, 117–134. https://doi.org/10.1080/00758914.2016.1193323

Langgut, D., Finkelstein, I., Litt, T., 2013. Climate and the Late Bronze Collapse: New Evidence from the Southern Levant. Tel Aviv 40, 149–175. https://doi.org/10.1179/033443513X13753505864205

Langgut, D., Finkelstein, I., Litt, T., Neumann, F., Stein, M., 2015. Vegetation and Climate Changes during the Bronze and Iron Ages (~3600 – 600 BCE) in the Southern Levant Based on Palynological Records. Radiocarbon 57, 217–235. https://doi.org/10.2458/azu

Langgut, D., Neumann, F., Stein, M., Wagner, A., Kagan, E., Bharetto, E., Finkelstein, I., 2014. Dead Sea Pollen Record and History of Human Activity in the Judean Highlands (Israel) from the Intermediate Bronze into the Iron Ages (~2500–500 BCE). Palynology 38, 280–302. https://doi.org/10.1080/01916122.2014.906001

Lingis, P., Michaelides, S., 2009. Teleconnection patterns of the Siberian Anticyclone and precipitation over Cyprus. Atmos. Res. 94, 663–674. https://doi.org/10.1016/j.atmosres.2009.05.013

Litt, T., Ohlwein, C., Neumann, F., Hense, A., Stein, M., 2012. Holocene climate variability in the Levant from the Dead Sea pollen record. Quat. Sci. Rev. 49, 95–105. https://doi.org/10.1016/j.quascirev.2012.09.017

López-Moreno, J., Vicente-serrano, S., Morán-tejeda, E., Lorenzo-Lacruz, J., Kenawy, A., Beniston, M., Instituto, A., 2011. Effects of the North Atlantic Oscillation (NAO) on combined temperature and precipitation winter modes in the Mediterranean mountains: Observed relationships and projections for the 21st century. Glob. Planet. Change 77, 62–76. https://doi.org/10.1016/j.gloplacha.2011.03.003

Margaritelli, G., Vallefuoco, M., Di Rita, F., Capotondi, L., Bellucci, L., Insinga, D., Petrosino, P., Bonomo, S., Cacho, I., Cascella, A., Ferraro,

L., 2016. Marine response to climate changes during the last five millennia in the central Mediterranean. Glob. Planet. Change 142, 53–72. https://doi.org/10.1016/j.gloplacha.2016.04.007

Martin, A., Harvey, W., 2017. The Global Pollen Project: a new tool for pollen identification and the dissemination of physical reference collections. Methods Ecol. Evol. 8, 892–897.

Mayewski, P., Rohling, E., Stager, J., Karlén, W., Maasch, K., Meeker, L., Meyerson, E., Gasse, F., van Kreveld, S., Holmgren, K., Lee-Thorp, J., Rosqvist, G., Rack, F., Staubwasser, M., Schneider, R., Steig, E., 2004. Holocene climate variability. Quat. Res. 62, 243–255. https://doi.org/10.1016/j.yqres.2004.07.001

McMichael, A., 2012. Insights from past millennia into climatic impacts on human health and survival. Proc. Natl. Acad. Sci. U. S. A. 109, 4730–4737. https://doi.org/10.1073/pnas.1120177109

Mora, D., Carmona, J., Jahn, R., Zimmermann, J., Abarca, N., 2017. Epilithic diatom communities of selected streams from the Lerma-Chapala Basin, Central Mexico, with the description of two new species. PhytoKeys 88, 39–69. https://doi.org/10.3897/phytokeys.88.14612

Morales, E., Fernández, E., Kociolek, P., 2009. Epilithic diatoms (Bacillariophyta) from cloud forest and alpine streams in Bolivia, South America 3: Diatoms from Sehuencas, Carrasco National Parkc, Department of Cochabamba. Acta Bot. Croat. 68, 263–283.

Morhange, C., Goiran, J., Bourcier, M., Carbonel, P., Le Campion, J., Rouchy, J., Yon, M., 2000. Recent Holocene paleo-environmental evolution and coastline changes of Kition, Larnaca, Cyprus, Mediterranean Sea. Mar. Geol. 170, 205–230. https://doi.org/10.1016/S0025-3227(00)00075-X

Neumann, J., Parpola, S., 1987. Climatic Change and the Eleventh-Tenth-Century Eclipse of Assyria and Babylonia. J. Near East. Stud. 46, 161–182.

Nigro, L., 2000. Coordinating the Middle Bronze Age I pottery chronol- ogy of Syria and Palestine., in: Matthiae, P. (Ed.), Proceedings of the First International Congress on the Archaeology of the Ancient Near East, Rome, May 18th–23rd 1998. pp. 1187–1210.

Ohtsuka, T., Kato, S., Asai, K., Watanabe, T., 2009. Checklist and illustrations of diatoms in Laguna de Bay, Philippines, with reference to

water quality. Diatom 25, 134–147. https://doi.org/10.11464/diatom.25.134

Olsen, J., Anderson, N., Knudsen, M., 2012. Variability of the North Atlantic Oscillation over the past 5,200 years. Nat. Geosci. 5, 808–812. https://doi.org/10.1038/ngeo1589

Otsuka, T., 2018. WEB Diatom Picture Book [WWW Document]. Lake Biwa Museum Res. Arch. Shiga Prefect. Kusatsu, Japan. URL https://www.biwahaku.jp/research/data/atlas/speciesname.html

PalDat – a palynological database [WWW Document], 2000. . Div. Struct. Funct. Bot. Univ. Vienna. URL www.paldat.org

Pantelas, V., 1996. The Cyprian bioclimate and the climax plant associations. Proc. 6th Sci. Conf. Hell. Bot. Soc. Paralimni Cyprus.

Poliakova, A., Behling, H., 2016. Pollen and fern spores recorded in recent and late Holocene marine sediments from the Indian Ocean and Java Sea in Indonesia. Quat. Int. 392, 251–314. https://doi.org/10.1016/j.quaint.2015.06.046

Potapova, M., Minerovic, A., Veselá, J., Smith, C., 2016. Diatom New Taxon File [WWW Document]. Acad. Nat. Sci. Drexel Univ. Philadelphia. URL http://symbiont.ansp.org/dntf/

Praglowski, J., 1962. Notes on the pollen morphology of swedish trees and shrubs. Grana Palynol. 3, 45–76. https://doi.org/10.1080/00173136209429099

Pullan, M., 2003. Automatic Diatom Identification And Classification Diatom Image Database [WWW Document]. R. Bot. Gard. Edinburgh. URL https://rbg-web2.rbge.org.uk/ADIAC/db/adiacdb.htm

R Core Team T, 2017. . R A Lang. Environ. Stat. Comput.

Reed, J., Stevenson, A., Juggins, S., Ne, T., 2001. A multi-proxy record of Holocene climatic change in southwestern Spain: the Laguna de Medina, Cadiz. The Holocene 6, 707–719.

Reichardt, E., 2011. Beitrag zur Diatomeenflora (Bacillariophyceae) des Paterzeller. Berichte der Bayer. Bot. Gesellschaft 81, 5–28.

Reimer, P., Bard, E., Bayliss, A., Beck, J., Blackwell, P., Ramsey, C., Buck, C., Cheng, H., Edwards, R., Friedrich, M., Grootes, P., Guilderson,

T., Haflidason, H., Hajdas, I., Hatté, C., Heaton, T., Hoffmann, D., Hogg, A., Hughen, K., Kaiser, K.F., Kromer, B., Manning, S., Niu, M., Reimer, R.W., Richards, D.A., Scott, E.M., Southon, J.R., Staff, R.A., Turney, C.S.M., van der Plicht, J., 2013. IntCal13 and Marine13 Radiocarbon Age Calibration Curves 0–50,000 Years cal BP. Radiocarbon 55, 1869–1887. https://doi.org/10.2458/azu_js_rc.55.16947

Renault-Miskovsky, J., 1985. Palynologie, in: Peltenburg, E. (Ed.), Lemba Archaeological Project I. Excavations at Lemba-Lakkous Vol. 70:1. Studies in Mediterranean Archaeology, Goteborg, pp. 306–311.

Renault-Myskovsky, J., 1989. Étude paléobotanique, paléoclimatique et palethnographique du site néolithique de Khirokitia à Chypre: rapport de la palynologie, in: La Brun, A. (Ed.), Fouilles Récent à Khirokitia (Chypre) - 1983-1986 Vol. 81. ADPF: Recherches sur les Civilisation, Memoire, Paris, pp. 251–276.

Riehl, S., Pustovoytov, K., Dornauer, A., Sallaberger, W., 2012. Mid-to-late Holocene agricultural system transformations in the northern Fertile Crescent: A review of the archaeobotanical, geoarchaeological, and philological evidence. Geophys. Monogr. Ser. 198, 115–136. https://doi.org/10.1029/2012GM001221

Rimbu, N., Lohmann, G., Kim, J.H., Arz, H.W., Schneider, R., 2003. Arctic/North Atlantic Oscillation signature in Holocene sea surface temperature trends as obtained from alkenone data. Geophys. Res. Lett. 30, 2000–2003. https://doi.org/10.1029/2002GL016570

Roberts, N., Eastwood, W., Kuzucuoğlu, C., Fiorentino, G., Caracuta, V., 2011. Climatic, vegetation and cultural change in the eastern Mediterranean during the mid-Holocene environmental transition. The Holocene 21, 147–162. https://doi.org/10.1177/0959683610386819

Roberts, N., Moreno, A., Valero-Garcés, B., Corella, J., Jones, M., Allcock, S., Woodbridge, J., Morellón, M., Luterbacher, J., Xoplaki, E., Türkeş, M., 2012. Palaeolimnological evidence for an east-west climate see-saw in the Mediterranean since AD 900. Glob. Planet. Change 84–85, 23–34. https://doi.org/10.1016/j.gloplacha.2011.11.002

Roberts, N., Woodbridge, J., Palmisano, A., Bevan, A., Fyfe, R., Shennan, S., 2019. Mediterranean landscape change during the Holocene: Synthesis, comparison and regional trends in population, land cover and climate. Holocene 29, 923–937. https://doi.org/10.1177/0959683619826697

Rohling, E., Mayewski, P., Abu-Zied, R., Casford, J., Hayes, A., 2002. Holocene atmosphere-ocean interactions: Records from Greenland and

the Aegean sea. Clim. Dyn. 18, 587–594. https://doi.org/10.1007/s00382-001-0194-8

Rosen, A., 2007. Civilising Climate. Social Responses to Climate Change in the Ancient Near East. Altamira Press.

Russell, J., Talbot, M., Haskell, B., 2003. Mid-holocene climate change in Lake Bosumtwi, Ghana. Quat. Res. 60, 133–141. https://doi.org/10.1016/S0033-5894(03)00065-6

Schilman, B., Ayalon, A., Bar-Matthews, M., Kagan, E., Almogi-Labin, A., 2002. Sea-land paleoclimate correlation in the Eastern Mediterranean region during the late Holocene. Isr. J. Earth Sci. 51, 181–190. https://doi.org/10.1560/504G-0017-5NKY-GUN1

Schloen, J.., 2017. Economic and Political Implications of Raising the Date for the Disappearance of Walled Towns in the Early Bronze Age Southern Levant, in: Höflmayer, F. (Ed.), The Late Third Millennium in the Ancient Near East. Chronology, C14 and Climate Change. The Oriental Institute of the University of Chicago, pp. 59–71.

Shore, J., Bartley, D., Harkness, D., 1995. Problems encountered with the 14C dating of peat. Quat. Sci. Rev. 14, 373–383. https://doi.org/10.1016/0277-3791(95)00031-3

Shubharani, R., Roopa, P., Sivaram, V., 2013. Pollen Morphology of Selected Bee Forage Plants. Glob. J. Bio-Science Biotechnol. 2, 82–90.

Solak, C., Kulikovskiy, M., Kaleli, A., Gönülol, A., 2016. Rare and new records of diatoms in Turkey from Kütahya flowing waters. Oceanol. Hydrobiol. Stud. 45, 564–587. https://doi.org/10.1515/ohs-2016-0047

Sorrel, P., Mathis, M., 2016. Mid- to late-Holocene coastal vegetation patterns in Northern Levant (Tell Sukas, Syria): Olive tree cultivation history and climatic change. The Holocene 26, 858–873. https://doi.org/10.1177/0959683615622555

Stebler, T., 2015. Pollen-Wiki – a Digital Pollen Atlas and Pollen Database [WWW Document]. URL http://pollen.tstebler.ch/MediaWiki/index.php?title=Pollenatlas:en

Stocchetti, E., Armanini, D., Angeli, N., Spitale, D., Cantonati, M., Kelly, M., Dörflinger, G., 2016. Analysis of riverine diatoms from Cyprus: a first overview of the assemblage composition and ecological status estimates. Not. dei Metod. Anal. 2, 90–99.

Sutula, M., Stein, E., Mazor, R., Theroux, S., Paul, M., Jessop, B., Gerritsen, J., Tech, T., 2016. Expert Interperetation of the Biological

Condition Gradient in California. Dev. a Biol. Cond. Gradient Model Calif. Wadeable Streams Oct, 1–26.

Swedish Meterological and Hydrological Institute, 2018. Nordic Microalgae and aquatic protozoa [WWW Document]. Swedish Meterological Hydrol. Inst. URL http://nordicmicroalgae.org/taxon/Gyrodinium spirale?media_id=Gyrodinium spirale_3.jpg

Tarasov, P., Cheddadi, R., Guiot, J., Bottema, S., Peyron, O., Belmonte, J., Ruiz-Sanchez, V., Saadi, F., Brewer, S., 1998. A method to determine warm and cool steppe biomes from pollen data; application to the Mediterranean and Kazakhstan regions. J. Quat. Sci. 13, 335–344. https://doi.org/10.1002/(SICI)1099-1417(199807/08)13:4<335::AID-JQS375>3.0.CO;2-A

Triantaphyllou, M., Gogou, A., Bouloubassi, I., Dimiza, M., Kouli, K., Rousakis, G., Kotthoff, U., Emeis, K., Papanikolaou, M., Athanasiou, M., Parinos, C., Ioakim, C., Lykousis, V., 2014. Evidence for a warm and humid Mid-Holocene episode in the Aegean and northern Levantine Seas (Greece, NE Mediterranean). Reg. Environ. Chang. 14, 1697–1712. https://doi.org/10.1007/s10113-013-0495-6

Van Geel, B., 1972. Palynology of a Section From the Raised Peat Bog 'Wietmarscher Moor', With Special Reference To Fungal Remains. Acta Bot. Neerl. 21, 261–284. https://doi.org/10.1111/j.1438-8677.1972.tb00779.x

Van Wichelen, J., Camelbeke, K., Chaerle, P., Goetghebeur, P., Huysmans, S., 1999. Comparison of different treatments for LM and SEM studies and systematic value of pollen grains in Cyperaceae. Grana 38, 50–58. https://doi.org/10.1080/001731300750044708

Vogiatzakis, Mannion, Sarris, 2016. Mediterranean island biodiversity and climate change: the last 10,000 years and the future. Biodivers. Conserv. 25, 2597–2627.

Wanner, H., Beer, J., Butikofer, J., Crowley, T., Cubasch, U., Fluckiger, J., Goosse, H., Grosjean, M., Joos, F., Kaplan, J., Kuttel, M., Muller, S., Prentice, I., Solominaj, O., Stocker, T., Tarasov, P., Wagner, M., Widmann, M., 2008. Mid- to Late Holocene climate change: an overview. Quat. Sci. Rev. 27, 1791–1828. https://doi.org/10.1016/j.quascirev.2008.06.013

Weiss, B., 1982. The Decline of Late Bronze Age Civilization as a Possible Response to Climatic Change. Clim. Chang. 4, 173–198.

Weiss, H., 2017. 4.2 ka BP Megadrought and the Akkadian Collapse, in: Megradrought and Collapse: From Early Agriculture to Angkor. Oxford University Press, pp. 93–160.

Weiss, H., 1997. Late third millennium abrupt climate change and social collapse in West Asia and Egypt, in: Dalfes, H., Kukla, G., Weiss, H. (Eds.), Third Millennium BC Climate Change and Old World Collapse. Springer, pp. 711–723.

Weiss, H., Courty, M., 1993. The genesis and collapse of the Akkadian Empire: the accidental refraction of historical law., in: Liverani, M. (Ed.), Akkad: The First World Empire: Structure, Ideology and Traditions. pp. 131–56.

Weiss, H., Courty, M., Wetterstrom, W., Guichard, F., Senior, L., Meadow, R., Curnow, A., 1993. The genesis and collapse of third millennium North Mesopotamian civilization. Science (80-.). 261, 995–1004.

Willard, D., Bernhardt, C., Cooper, S., 2004. Atlas of Pollen and Spores of the Florida Everglades. Palynology 28, 175–227.

Woodbridge, J., Roberts, N., 2011. Late Holocene climate of the Eastern Mediterranean inferred from diatom analysis of annually-laminated lake sediments. Quat. Sci. Rev. 30, 3381–3392. https://doi.org/10.1016/j.quascirev.2011.08.013

Yildiz, K., 2006. Morphological and palynological investigation on Silene gigantea L. var. gigantea and Silene behen L. (Caryophyllaceae) distributed in Western Anatolia and Northern Cyprus. Turk. J. Botany 30, 105–119.

Yildiz, K., Gucel, S., Dadandi, M., 2009. A Palynological Investigation of Endemic Taxa from Northern Cyprus. Pakistani J. Bot. 41, 991–1007.

Table 1. Raw and calibrated radiocarbon ages for cores AM18-1 and AM18-5. Ages were calibrated using the IntCal13 calibration curve (Reimer et al., 2013) and 95.4% ranges shown. Upper section displays the dates utilised in the age model, lower section displays the discounted dates.

Lab Number	Core	Depth (cm)	Unit	Dated material	Raw radiocarbon age (^{14}C yr BP)	Calibrated age range (cal yr BP)	Mean calibrated age (cal yr BP)	Archaeological Phase
GdA-5779	1	37-40	4a	Bulk sediment	1565 ± 30	1361 – 1586	1466	Byzantine
GdA-5634	1	100	6	Wood fragment	3260 ± 30	3384 – 3601	3489	Late Cypriot IB

GdA-5872	1	136	7	Peaty wood	4090 ± 30	4455 – 4807	4594	Late Chalcolithic
GdA-5868	5	21.5-23	6	Bulk organic sediment	1610 ± 25	1384 – 1603	1487	Byzantine
GdA-5869	5	46-48	6	Bulk organic sediment	2775 ± 45	2741 – 3057	2873	Cypro-Geometric II
GdA-5870	5	74-76	6	Bulk organic sediment	4210 ± 40	4549 – 4909	4737	Late Chalcolithic

GdA-5664	1	40	4a	Large root	-325 ± 30	-6.2 – -59.5	-26.3
GdA-5871	1	81-84	6	Bulk organic sediment	4095 ± 55	4822 – 4442	4619
GdA-6010	1	85	6	Bulk organic sediment	4250 ± 30	4864 – 4708	4786
GdA-6011	1	115	7	Bulk organic sediment	2185 ± 40	2355 – 2156	2256
GdA-6013	5	68	6	Bulk organic sediment	-237 ± 50	-5.4 – -6.4	-5.9

Figure Captions:

Figure 1. Location of the Akrotiri Marsh within the context of (A) Cyprus and (B) Akrotiri Peninsula; (C) Coring locations on the Akrotiri Marsh. Images from Google Earth.

Figure 2. Stratigraphy and radiocarbon age-depth diagrams for cores AM18-1 and AM18-5. Age models produced using the Bacon package in R (Blaauw and Christen, 2019), with ages calibrated using the IntCal13 calibration curve and reported with 95.4% confidence intervals (see sections 3 and 4.1).

Figure 3. Pollen ecology summary diagram for core AM18-1 plotted against depth, age and archaeological periods. Expanded section shows the Bronze Age interval in higher resolution. The archaeological phases of Knapp (2008), Knapp (2013), and Kearns and Manning (2019) are used for providing archaeological context to the palaeoenvironmental results (*Supplementary Table S1*).

Figure 4. Pollen ecology summary diagram for core AM18-5 plotted against depth, age and archaeological periods. The archaeological phases of Knapp (2008), Knapp (2013), and Kearns and Manning (2019) are used for providing archaeological context to the palaeoenvironmental results (*Supplementary Table S1*).

Figure 5. Summary of diatoms from core AM18-1 by ecological preference. Ecological categories are explained as follows: **Sensitivity** value assigned depending on the concentration of filterable reactive nutrients (phosphorous) at which the taxa were most abundant, after Kelly et al. (1995), with category 1 indicating greatest sensitivity to the presence of phosphorous: category 1 <0.01 mg/l; category 2 ≥0.01, <0.035 mg/l; category 3 ≥0.035, <0.1 mg/l; category 4 ≥0.1, <0.3 mg/l; category 5 ≥0.3 mg/l. **Moisture** classified as category 1 = never, or only very rarely, occurring outside water bodies; category 2 = mainly occurring in water bodies, sometimes on wet places; category 3 = mainly occurring in water bodies and also regularly on wet or moist places; category 4 = mainly occurring on wet, moist or temporarily dry places; category 5 = nearly exlcusively occurring outside water bodies (Van Dam et al., 1994). **Biological Condition Gradient (BCG)** describes changes in aquatic systems across increasing levels of human disturbance, whereby category 1 = environmentally specialist species requiring a natural environment; category 2 = highly sensitive species – similar to a natural environment; category 3 = sensitive species – slight alteration of natural environment leads to a loss of highly sensitive species; category 4 = indiscriminate species – moderate changes to natural environment lead to replacement of some sensitive ubiquitous taxa by more tolerant taxa; category 5 = tolerant species – high level of changes to natural environment lead to a marked reduction in sensitive taxa, conspicuously unbalanced taxonomic distribution and reduced complexity; category 6 = anthropogenic specialist species (Davies et al., 2006; Sutula et al., 2016). Classification of diatoms by salinity, pH, trophic state, nitrogen uptake, oxygen saturation and saprobity taken from Vos et al. (1993), Van Dam et al. (1994) and Denys (1992).

Figure 6. Summary of diatoms from core AM18-5 by ecological preference (for explanation of categories used, see Fig. 5 caption).

Figure 7. Synthesis of all proxy records showing fossil pollen and diatom derived key water availability intervals alongside archaeological periods, Bronze Age configuration of the dominant North Atlantic Oscillation (NAO) (Olsen et al., 2012; Margaritelli et al., 2016; Di Rita et al., 2018) and increased intensity Siberian High intervals (Rohling et al., 2002; Mayewski et al., 2004). Archaeological end date for Alassa *Paleotaverna* from Knapp (2013). The archaeological phases of Knapp (2008), Knapp (2013), and Kearns and Manning (2019) are used for providing archaeological context to the palaeoenvironmental results (*Supplementary Table S1*).

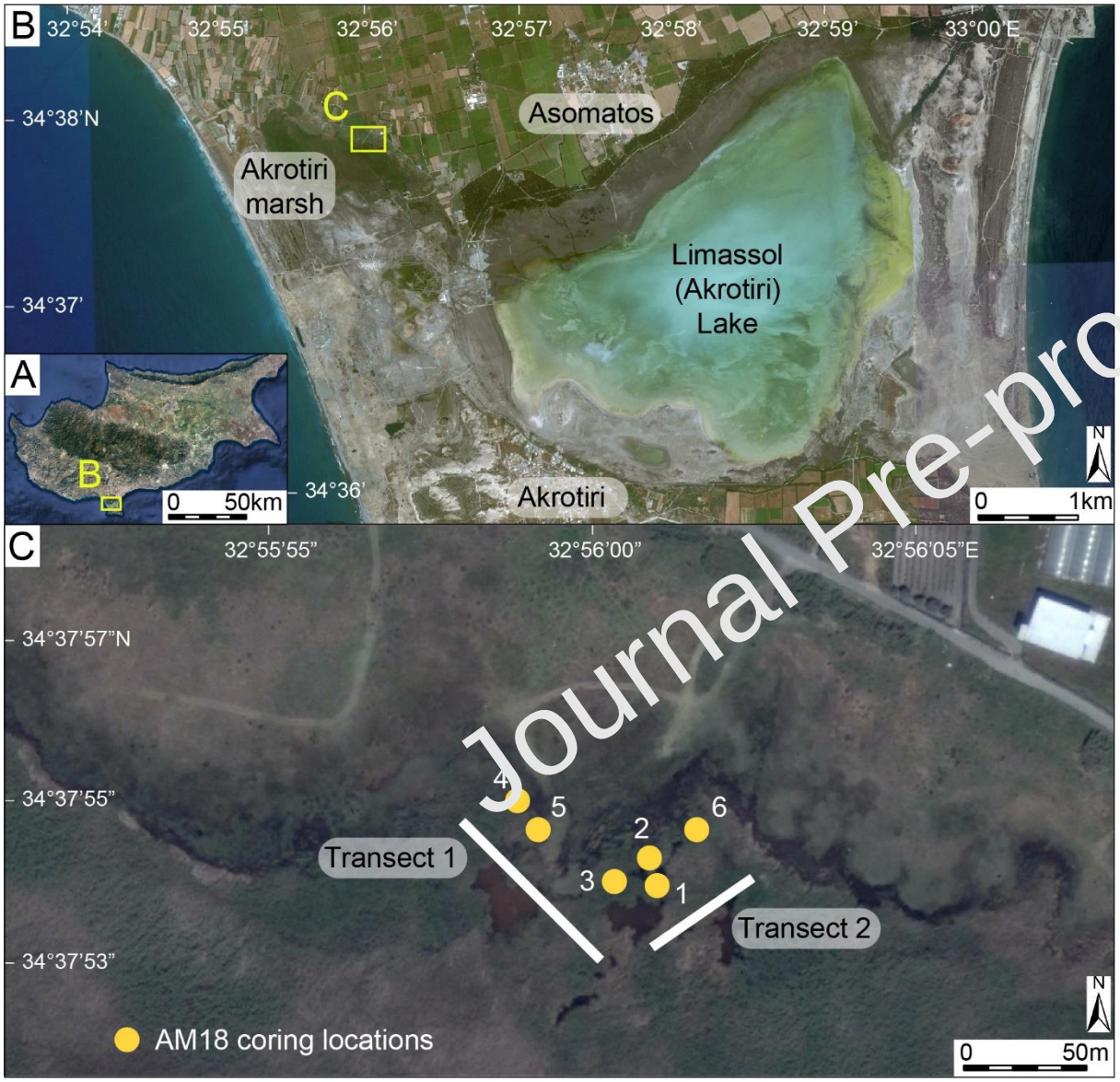

Figure 1. Location of the Akrotiri Marsh within the context of (A) Cyprus and (B) Akrotiri Peninsula; (C) Coring locations on the Akrotiri Marsh. Images from Google Earth.

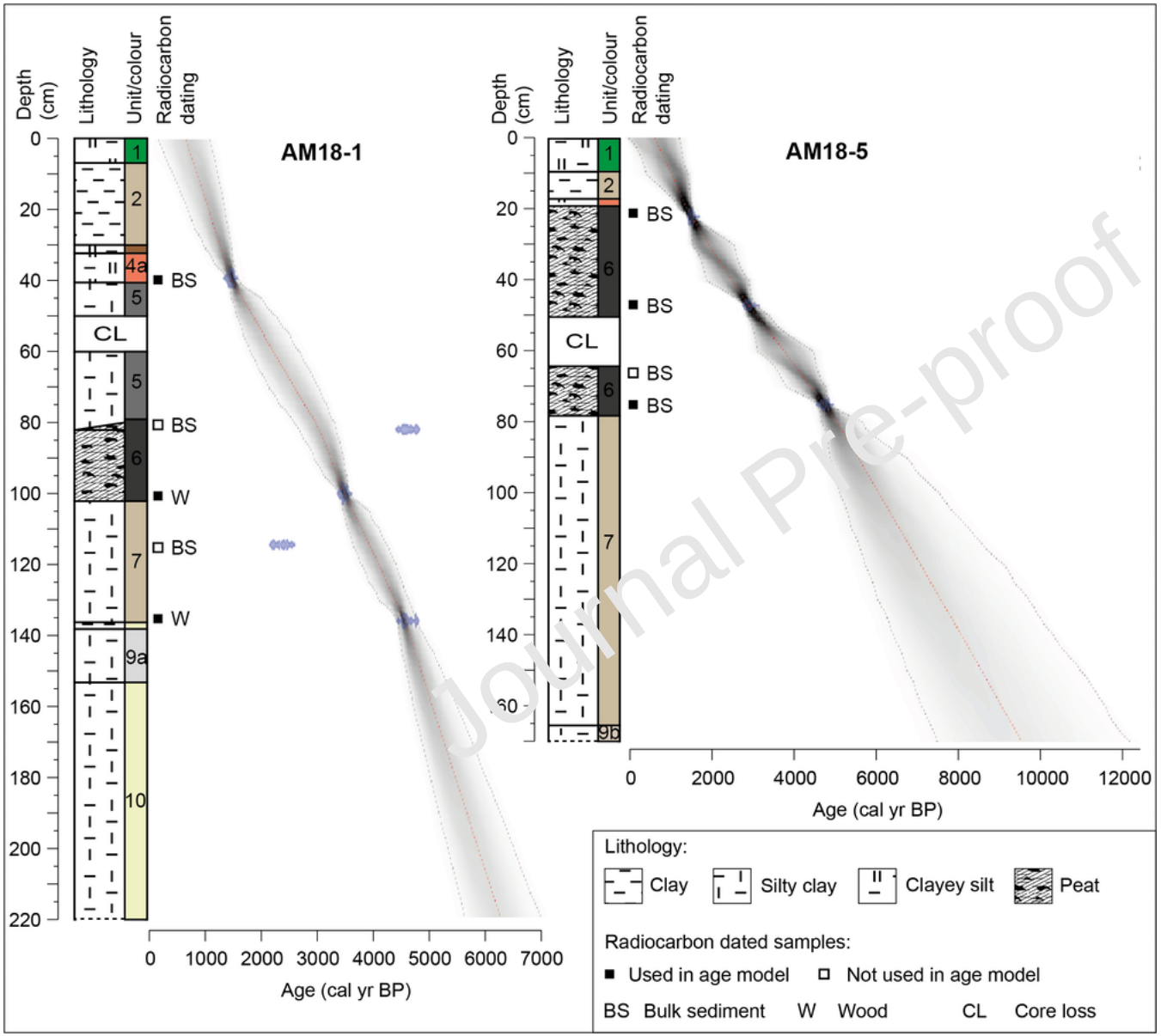

Figure 2. Stratigraphy and radiocarbon age-depth diagrams for cores AM18-1 and AM18-5. Age models produced using the Bacon package in R (Blaauw and Christen, 2019), with ages calibrated using the IntCal13 calibration curve and reported with 95.4% confidence intervals (see sections 3 and 4.1).

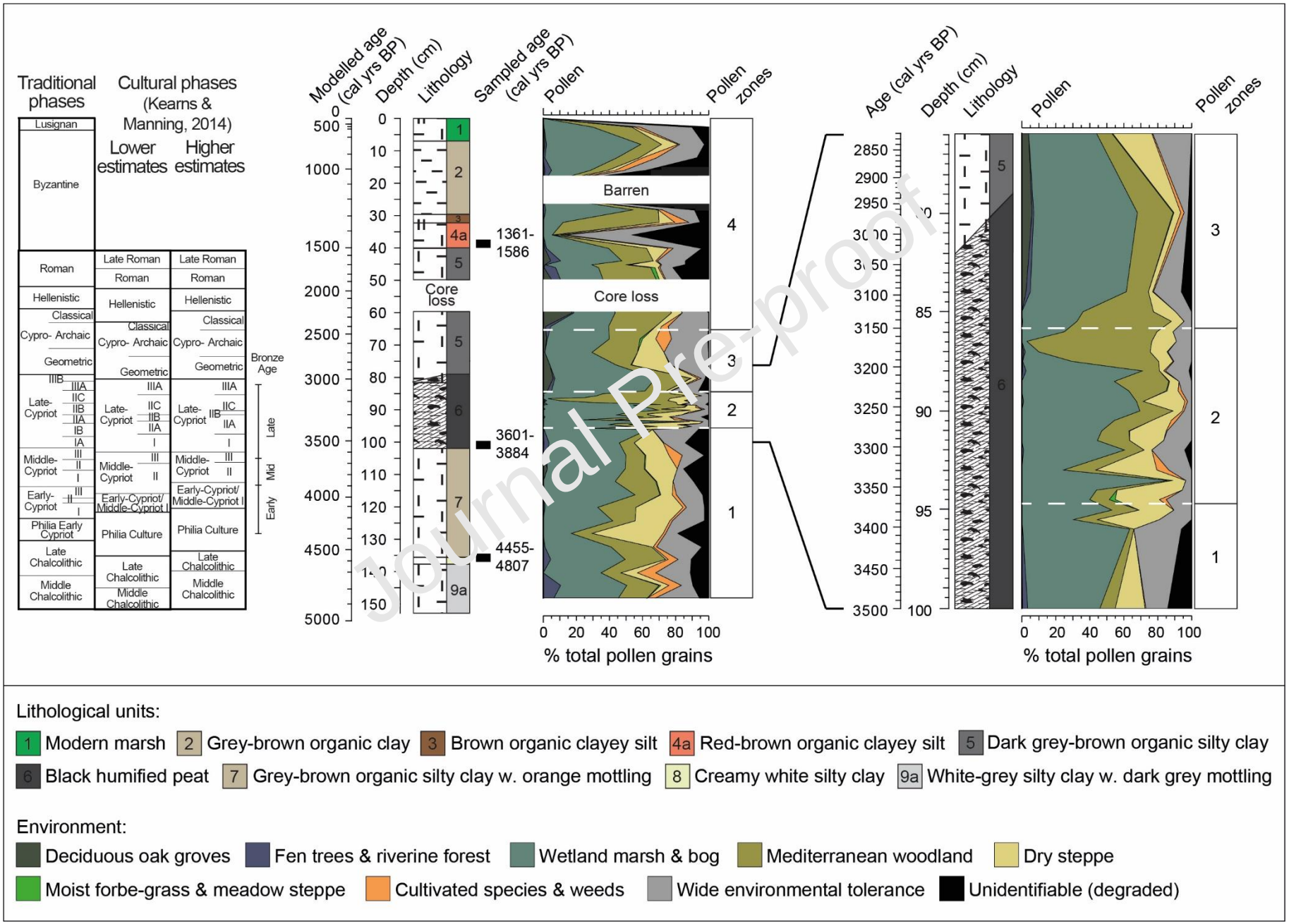

Lithological units:

1 Modern marsh | 2 Grey-brown organic clay | 3 Brown organic clayey silt | 4a Red-brown organic clayey silt | 5 Dark grey-brown organic silty clay | 6 Black humified peat | 7 Grey-brown organic silty clay w. orange mottling | 8 Creamy white silty clay | 9a White-grey silty clay w. dark grey mottling

Environment:

Deciduous oak groves | Fen trees & riverine forest | Wetland marsh & bog | Mediterranean woodland | Dry steppe | Moist forbe-grass & meadow steppe | Cultivated species & weeds | Wide environmental tolerance | Unidentifiable (degraded)

Figure 3. Pollen ecology summary diagram for core AM18-1 plotted against depth, age and archaeological periods. Expanded section shows the Bronze Age interval in higher resolution. In this paper the archaeological phases of Knapp (2008), Knapp (2013), and Kearns and Manning (2019) are used for providing archaeological context to the palaeoenvironmental results (*Supplementary Table S1*).

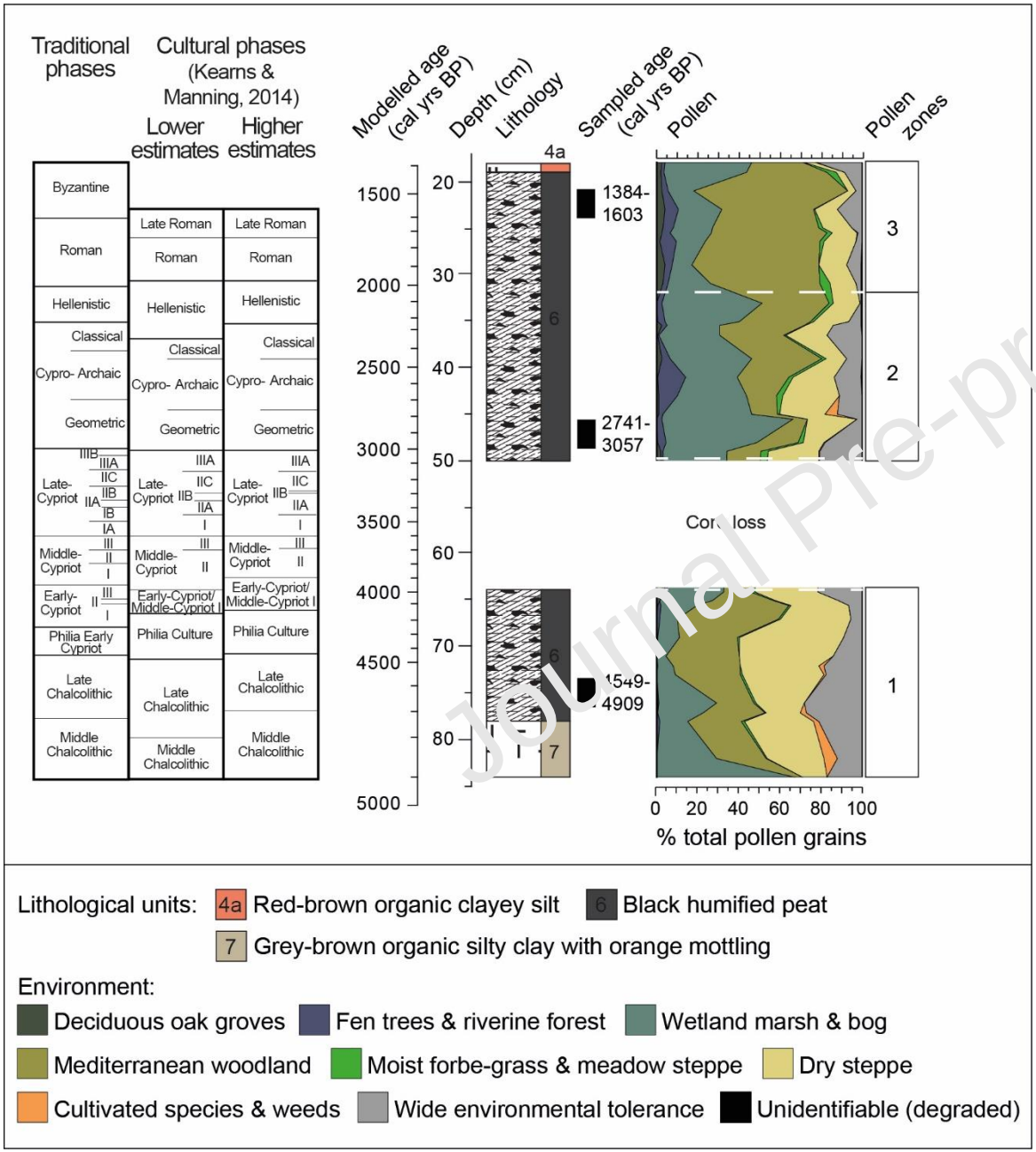

Figure 4. Pollen ecology summary diagram for core AM18-5 plotted against depth, age and archaeological periods. In this paper the archaeological phases of Knapp (2008), Knapp (2013), and Kearns and Manning (2019) are used for providing archaeological context to the palaeoenvironmental results (*Supplementary Table S1*).

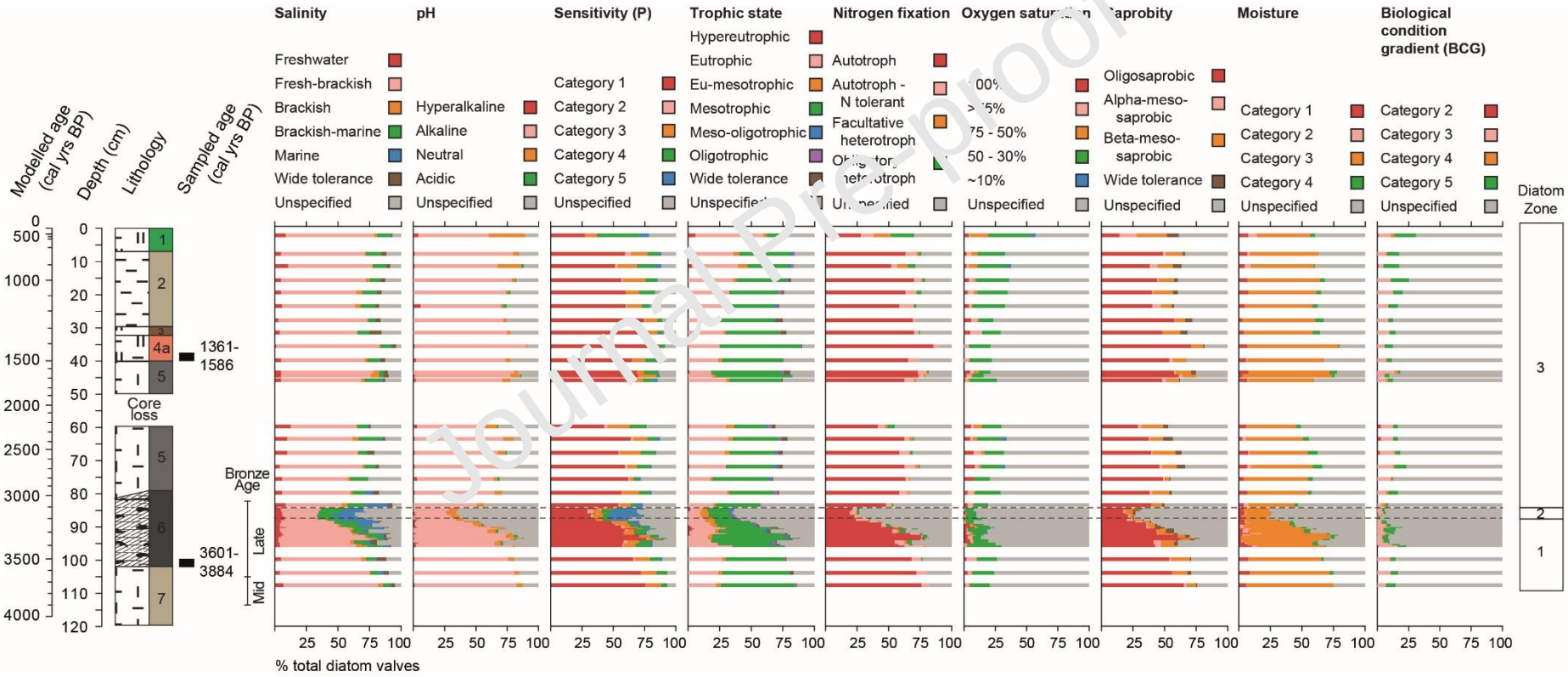

Figure 5. Summary of diatoms from core AM18-1 by ecological preference. Ecological categories are explained as follows: **Sensitivity** value assigned depending on the concentration of filterable reactive nutrients (phosphorous) at which the taxa were most abundant, after Kelly et al.

(1995), with category 1 indicating greatest sensitivity to the presence of phosphorous; category 1 <0.01 mg/l; category 2 ≥0.01, <0.035 mg/l; category 3 ≥0.035, <0.1 mg/l; category 4 ≥0.1, <0.3 mg/l; category 5 ≥0.3 mg/l. **Moisture** classified as category 1 = never, or only very rarely, occurring outside water bodies; category 2 = mainly occurring in water bodies, sometimes on wet places; category 3 = mainly occurring in water bodies and also regularly on wet or moist places; category 4 = mainly occurring on wet, moist or temporarily dry places; category 5 = nearly exlcusively occurring outside water bodies (Van Dam et al., 1994). **Biological Condition Gradient (BCG)** describes changes in aquatic systems across increasing levels of human disturbance, whereby category 1 = environmentally specialist species requiring a natural environment; category 2 = highly sensitive species - similar to a natural environment; category 3 = sensitive species – slight alteration of natural environment leads to a loss of highly sensitive species; category 4 = indiscriminate species – moderate changes to natural environment lead to replacement of some sensitive ubiquitous taxa by more tolerant taxa; category 5 = tolerant species - high level of changes to natural environment lead to a marked reduction in sensitive taxa, conspicuously unbalanced taxonomic distribution and reduced complexity; category 6 = anthropogenic specialist species (Davies et al., 2006; Sutula et al., 2016). Classification of diatoms by salinity, pH, trophic state, nitrogen uptake, oxygen saturation and saprobity taken from Vos et al. (1993), Van Dam et al. (1994) and Denys (1992).

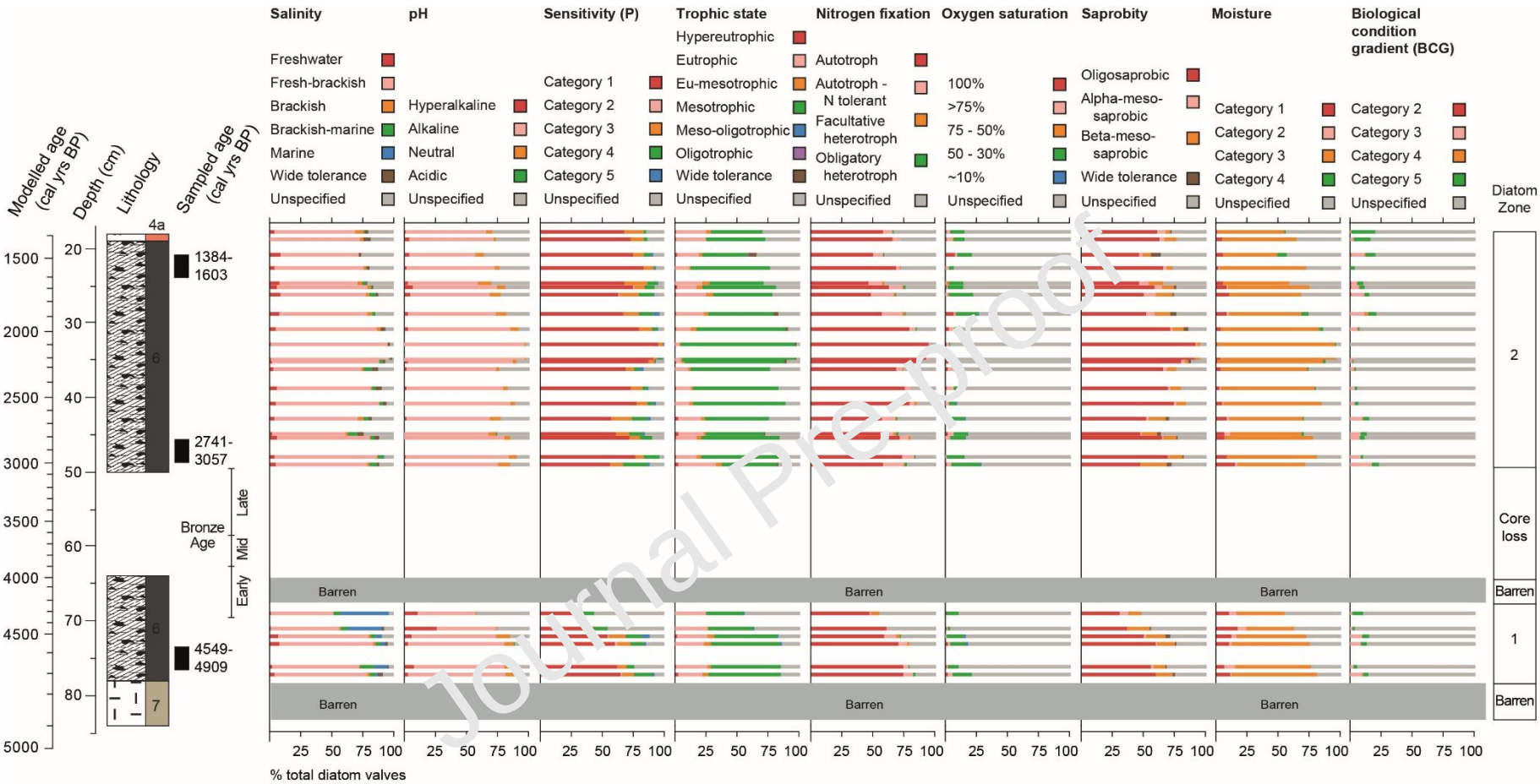

Figure 6. Summary of diatoms from core AM18-5 by ecological preference (for explanation of categories used, see Fig. 5 caption).

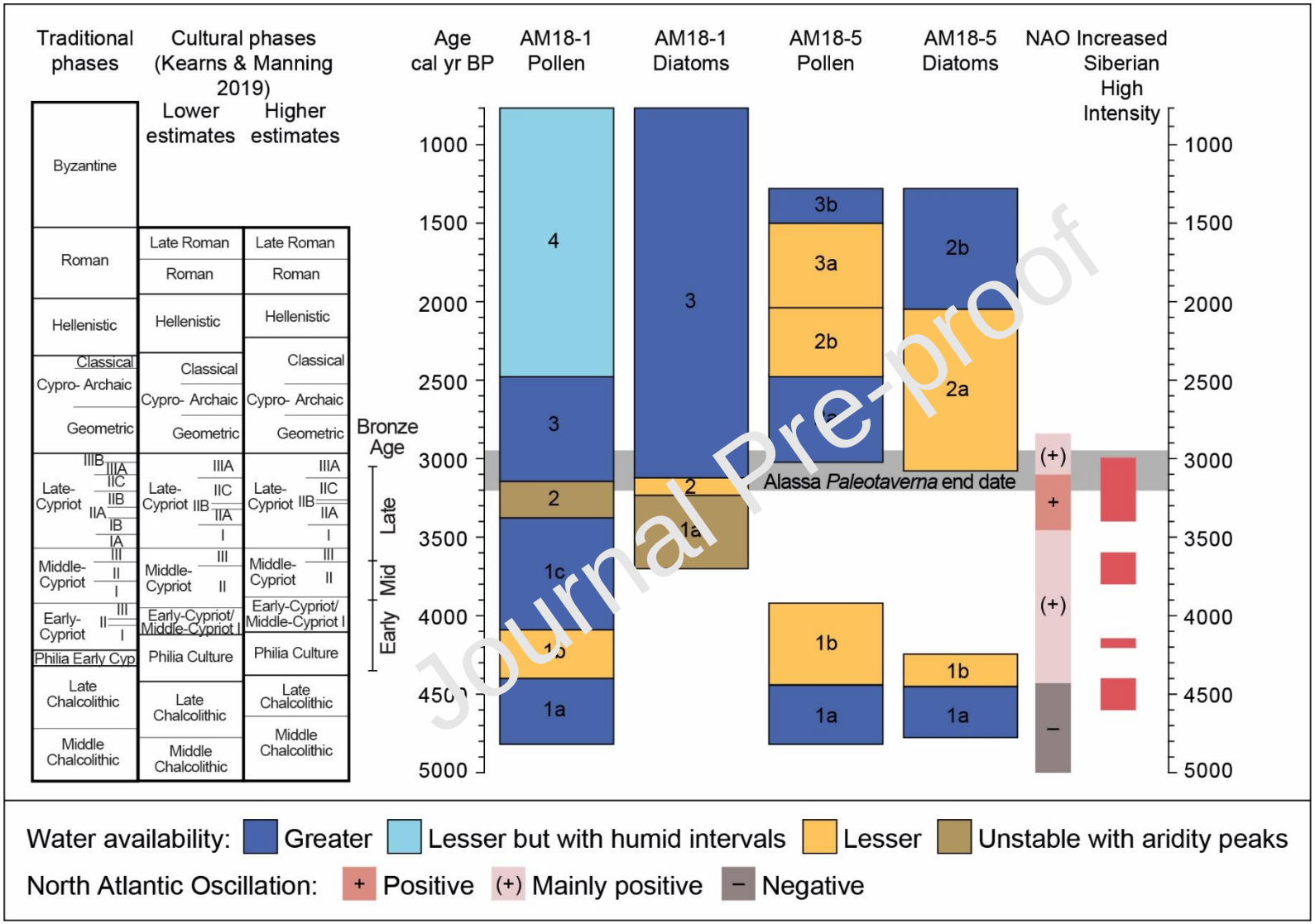

Figure 7. Synthesis of all proxy records showing fossil pollen and diatom derived key water availability intervals alongside archaeological periods, Bronze Age configuration of the dominant North Atlantic Oscillation (NAO) (Olsen et al., 2012; Margaritelli et al., 2016; Di Rita et al., 2018) and increased intensity Siberian High intervals (Rohling et al., 2002; Mayewski et al., 2004). Archaeological end date for Alassa *Paleotaverna* from Knapp (2013). In this paper the archaeological phases of Knapp (2008), Knapp (2013), and Kearns and Manning (2019) are used for providing archaeological context to the palaeoenvironmental results (*Supplementary Table S1*).

Declaration of interests

The authors declare that they have no known competing financial interests or personal relationships that could have appeared to influence the work reported in this paper.

Highlights

- Two 5000-year-old multiproxy records from the Akrotiri Marsh, southern Cyprus
- Both the 4.2K and 3.2K climate events had an impact on the island's water balance
- Pollen & diatoms infer Early Bronze Age peak aridity between 4.3 & 4.1 cal ka BP
- Repeat dry intervals in Late Bronze Age from 3.4 to 3.1 cal ka BP, W-Shaped event
- Insight into the expression of the North Atlantic Oscillation and the Siberian High